Student thesis series INES nr 585

Testing aerosol vertical profiling methods with portable instruments on unmanned and manned aircraft

Ellen Soroka

2023
Department of
Physical Geography and Ecosystem Science
Lund University
Sölvegatan 12
S-223 62 Lund
Sweden

Ellen Soroka (2023)
Testing aerosol vertical profiling methods with portable instruments on unmanned and manned aircraft
Master degree thesis, 30 credits in *Atmospheric Science & Biogeochemical Cycles*
Department of Physical Geography and Ecosystem Science, Lund University

Level: Master of Science (MSc)

Course duration: *January* 2022 until *January* 2023

Disclaimer

This document describes work undertaken as part of a program of study at the University of Lund. All views and opinions expressed herein remain the sole responsibility of the author, and do not necessarily represent those of the institute.

Testing aerosol vertical profiling methods with portable instruments on unmanned and manned aircraft

---

Ellen Soroka

Master thesis, 30 credits, in
Atmospheric Science & Biogeochemical Cycles

Supervisors:

Erik Ahlberg
Division of Nuclear Physics, Lund University

Vilhelm Malmborg
Department of Design Sciences, LTH

Vaughan Phillips
Department of Physical Geography and Ecosystem Science, Lund University

Exam committee:

Thomas Holst
Department of Physical Geography and Ecosystem Science, Lund University

Zhengyao Lu
Department of Physical Geography and Ecosystem Science, Lund University

Acknowledgements

I would like to warmly express my gratitude to my supervisors Erik Ahlberg and Vilhelm Malmborg for their encouragement and patience in guiding me through this project. Thank you also to my co-supervisor Vaughan Phillips.

This project would not have been possible without individuals from the Lund University School of Aviation: thank you to Rohith Prem Maben and Björn Wallinius for piloting the UAV, and to Rikard Tyllström, Joel Sköld, and Thomas Hallström for helping coordinate the UAV and plane flights.

Thank you for the feedback from my opponent and examiners. I am also grateful to the many individuals from the aerosol division and beyond who have shown interest and support in this project.

I also kindly acknowledge Naneos, Aethlabs, Alphasense, and Sparv Embedded for correspondence regarding instruments. Additional thanks to NOAA (National Oceanic and Atmospheric Administration) Air Resources Laboratory for the provision of the HYSPLIT (Hybrid Single-Particle Lagrangian Integrated Trajectory) transport and dispersion model and READY (Real-time Environmental Applications and Display sYstem) website (www.ready.noaa.gov) used in this publication.

Abstract

This thesis employed several portable sensors on board an unmanned aerial vehicle (UAV) and manned aircraft in order to test new methods of measuring vertical profiles of aerosol particles and contribute to knowledge of aerosol distributions in the atmosphere. More data in this area is required to improve atmospheric modelling and future climate scenarios. The handheld nanoparticle detector Partector 2, miniature aethalometer MA300, low-cost optical particle counter (OPC)-N3, and the portable aerosol spectrometer 11-D were used to measure the total number concentration of nanoparticles, the mass concentration of black carbon (BC), and the PM2.5 mass concentration. At the rural background monitoring site Hyltemossa, sensors compared well to reference instruments in most cases and a total of seven vertical profiles up to a maximum altitude of 165 m were performed with the UAV over two days (10-11th October 2022). Measurements were conducted both within/above the forest canopy and over a nearby cleared area, but no evidence was found to suggest that the canopy directly influenced the vertical aerosol distribution. However, notable differences in the resulting concentration profiles were observed between the two days, which could be linked to different air mass origins. During measurements onboard two manned instructional flights (operated by the Lund School of Aviation based in Ljungbyhed) on the 13th October, similar vertical profiles were observed during ascent and descent, despite over 200 km separation. A notable reduction in aerosol concentrations was observed from around 1500 m altitude, suggesting the plane crossed the planetary boundary layer (PBL). The methods used in this thesis were considered viable with a few improvements, such as a dryer for UAV-based sensors and a better sampling inlet for aircraft measurements. Using UAVs and instructional aircraft as platforms for portable sensors are promising techniques for regular vertical profile measurements, and future campaigns are expected to further increase understanding of aerosol distributions and related atmospheric processes.

Table of Contents

List of Abbreviations

ACTRIS	Aerosol, Clouds and Trace Gases Research Infrastructure
ANOVA	Analysis of Variance
AR6	Sixth Assessment Report (on Climate Change from IPCC)
BC	Black Carbon
BLH	Boundary Layer Height
CMIP	Coupled Model Intercomparison Project
DV	Deposition Voltage
HYSPLIT	Hybrid Single-Particle Lagrangian Integrated Trajectory
ICOS	Integrated Carbon Observation System
IRBC	Infrared Black Carbon
IPCC	Intergovernmental Panel on Climate Change
LDSA	Lung Deposited Surface Area
LiDAR	Light Detection And Ranging
LUSA	Lund University School of Aviation
MPSS	Mobility Particle Size Spectrometer
OPC	Optical Particle Counter
PBL	Planetary Boundary Layer
PM	Particulate Matter
PSD	Particle Size Distribution
PSL	Polystyrene Spherical Latex Particles
RH	Relative Humidity
RI	Refractive Index
STP	Standard Temperature and Pressure
UAV	Unmanned Aerial Vehicle
VP	Vertical Profile

Chapter 1

Introduction

The term aerosol collectively refers to a gas and the particles suspended therein (Hinds, 1982). These aerosol particles are known to have complex effects on both human health as well as the Earth's climate, with ongoing research striving to better understand and quantify aerosol-associated interactions and consequences. Studying the distributions and characteristics of atmospheric aerosol particles is particularly important because of the role they play in cloud microphysics and the radiation budget (Corrigan et al., 2008; Boucher, 2015), and thus relevant to understanding their role in climate change feedbacks and predicting future scenarios. In 2001, the Third Assessment Report from the Intergovernmental Panel on Climate Change (IPCC) highlighted that lack of data available to evaluate the vertical distribution of aerosol concentrations in models and constrain the large inter-model differences (Penner et al., 2021). 20 years later, the Sixth Assessment Report (AR6) reported that significant uncertainties regarding aerosol-cloud-radiation interactions still remain (Chen et al., 2021). These uncertainties are many and diverse, but one example hindering the aerosol radiative forcing estimation is the inadequate knowledge of aerosol vertical distributions (Reddy et al., 2013; Ferrero et al., 2014; Mishra et al., 2015; Molero et al., 2021).

On the global scale, observations of aerosol vertical profiles are lacking and, as a result, are represented in different models with high variability (Kipling et al., 2016). Aerosol properties are typically monitored over time by ground or near-ground stationary instruments which can already be limited by low horizontal spatial resolution, in part due to the high cost of purchasing and maintaining reference-grade instruments (Villa et al., 2016). Vertical profiles in the troposphere can be resolved with remote sensing technology such as LiDAR (Light Detection And Ranging), although this can also be limited by spatial resolution, high costs, and sensitivity to meteorological conditions (X. Li et al., 2018). Furthermore, this method is not sufficient for measuring the variation of aerosol mass concentration, particle size distribution (PSD), and chemical composition of particles within the vertical profile of the atmosphere (Corrigan et al., 2008; B. Liu et al., 2020).

Unmanned aerial vehicles (UAVs), commonly known as drones, can overcome some of these limitations. Cost efficiency, flexibility, and mobility are some of the benefits attributed to UAVs used for the measurement of atmospheric aerosols when combined with the continually improving range of small, portable, and, in some cases, low-cost aerosol sensors (Chiliński et al., 2018; Z. Liu et al., 2021; Wu et al., 2021). Utilising these sensors in UAV vertical measurements is a valuable opportunity to gather information on atmospheric aerosols. Even so, this method is not without its own challenges, such as payload and battery limitations, and airspace restrictions. Manned aircraft fitted with

these portable sensors present an additional possibility for measuring aerosols in the vertical column up to higher altitudes and for longer periods. Lund University School of Aviation's (LUSA) collaboration with other research divisions of the university provides a unique opportunity to involve instructional aircraft, as well as UAVs from their drone lab, in measurement campaigns.

1.1 Aims and Hypothesis

The focus of this thesis project was to contribute to knowledge of aerosol vertical profiles, including the means of measuring aerosol concentrations in the vertical column. The aims of the project were:

- To verify the data from portable aerosol sensors against near-ground measurements at the ACTRIS (Aerosol, Clouds and Trace Gases Research Infrastructure) regional background station Hyltemossa.
- To determine if these sensors are suitable for UAV- and plane-based aerosol vertical profiling and the feasibility of such campaigns.
- To measure how aerosol particles are vertically distributed in the planetary boundary layer (PBL) and the lower free troposphere.

A specific hypothesis that vertical profiles performed within/above the forest canopy differ from those performed in an open area was tested.

Chapter 2

Background

2.1 Atmospheric aerosols

Aerosol particles, or particulate matter (PM), vary in size from the nanometer scale to several tens of microns (Hinds, 1982). The sources of aerosols in the atmosphere are many and diverse, but broadly the aerosols can be classified in relation to their origin as either primary or secondary particles. Primary particulate matter is emitted directly to the atmosphere, while secondary particles form in the atmosphere from precursor gases which condense onto pre-existing particles, or form new particles through nucleation (Boucher, 2015). Both categories include numerous contributions from natural and anthropogenic processes, such as combustion (e.g. biomass combustion in wildfires or fossil fuel burning), events inducing the suspension of particles (e.g. wind-borne dust or road dust resulting from traffic). New particles can form from precursor gases emitted from industrial processes, or from biogenic volatile organic compounds such as isoprene and monoterpene emitted by forests which oxidise in the atmosphere to form secondary organic aerosols Mahilang et al., 2021.

2.1.1 Aerosols and climate

Aerosol particles interact in the atmosphere in complex ways and consequently there is a high degree of uncertainty surrounding their effects on radiative forcing and aerosol-cloud interactions (Z. Liu et al., 2021). Atmospheric aerosols have a notable influence on the climate in two main ways: causing perturbations to the global energy balance, and affecting the formation and properties of clouds (Boucher, 2015; Ferrero et al., 2014).

Global climate models indicate that atmospheric aerosols have a net cooling effect on the climate as they increase the Earth's total albedo and reflect solar radiation away from the surface (IPCC, 2013). However, some particles do have the opposite effect and contribute to the warming of the climate, namely carbonaceous particles such as black carbon (BC) which is a strongly absorbing substance (Ferrero et al., 2014; Wu et al., 2021). Quantifying concentrations and variations of both the absorbing and scattering aerosols in the atmosphere — and not just at ground-level — is vital for understanding the effect on radiative forcing and associated direct and indirect climate effects (Chilinski et al., 2016; Ran et al., 2016; Wu et al., 2021).

Aerosols affect cloud properties including cloud droplet size and concentration through their role as cloud condensation nuclei, in which water vapour condenses on certain particles (Fan et al., 2016). The higher the number of aerosol particles, the more cloud

droplets can form, but the smaller they will be. Referred to as the indirect aerosol effect, clouds formed amongst high aerosol concentrations are brighter and have longer lifetimes, thereby having a cooling effect with increased solar reflection. Clouds in turn also influence atmospheric aerosol numbers and size distribution, through wet deposition and in-cloud processing (Boucher, 2015).

2.1.2 Vertical distribution of aerosols

As a result of varying sources, meteorological conditions, and atmospheric processes and reactions, the characteristics of aerosols, and their distribution in the vertical direction, can vary significantly. Vertical profiles will vary depending on the property being measured (Cappelletti et al., 2022), as well as over time (Shi et al., 2020) and with geographic location (Heald et al., 2011). These factors and the many complex processes involved make it difficult to make generalised statements about the expected shape of a vertical profile in the entire atmosphere. Processes which can contribute to the vertical distribution of aerosol particles include convective transport, in- and below-cloud scavenging, growth by condensation, dry deposition, emission characteristics, and mixing within the PBL (Kipling et al., 2016).

The PBL refers to the lowest layer of the troposphere which is directly affected by wind variations, turbulence, and convective activity influenced by the surface of the Earth via surface friction, topography, and radiative heating (Quan et al., 2012; Boucher, 2015). The thickness of this layer, i.e. the BLH varies both diurnally and seasonally with meteorological conditions from roughly 100 to 2000 m (Boucher, 2015). The BLH is lowest during stable nights with low temperatures and minimal winds, while the maximum occurs when insolation is high and advection is strong, causing less stable air (Shi et al., 2020). Since the layer caps the air below with little transport across it into the free troposphere, the height of the PBL affects the concentration of aerosols close to the surface. It effectively compresses or expands the volume of air, thereby respectively increasing or decreasing the concentration of particles within the layer (Z. Li et al., 2017). Models often assume aerosols are homogeneously distributed within the PBL due to well-mixed air (Z. Li et al., 2017). However, measurements have shown that vertical concentrations may also decrease with height or inversely increase with altitude (Su et al., 2020).

Above the PBL in the free troposphere, the Earth-atmosphere interaction is reduced (Boucher, 2015). Since the bulk of aerosols are emitted and capped within the PBL, there is usually a sharp decrease in concentrations when crossing into the free troposphere (Shao et al., 2020). However, inversion, residual, and persistent layers can also be featured in tropospheric vertical profiles (Shao et al., 2020; Quan et al., 2012). Since the reduced friction in the free troposphere allows for higher wind speeds, long-range transport of particulate matter is more efficient and therefore the vertical profile can be influenced

by both local sources and air-masses carrying aerosols over long-distances (Cappelletti et al., 2022). This transport can be to the extent that mineral dust originating in Asia has been recorded circuiting the globe in about 13 days (Uno et al., 2009; Allen et al., 2021).

2.2 Measurements of aerosols in the vertical profile

In the first attempt to quantify how aerosol properties, in this case the number of dust particles, changes with altitude, Aitken (1890) carried a self-made portable 'dust-detective' apparatus to the top of the 300 m Eiffel tower prior to its inauguration. Measurements at altitude have since evolved with the use of radiosondes, satellites, balloons, manned aircraft, and most recently, UAVs.

2.2.1 Aircraft-based aerosol measurements

Using manned aircraft to obtain information about aerosol concentrations at different altitudes brings the benefits of being able to reach high altitudes, high tolerance to varied weather conditions, and the capacity to carry heavier and/or larger instruments. If the planes are being flown for reasons other than aerosol research (such as commercial or instructional flights) then installing aerosol instruments on board takes advantage of regular measurement opportunities, and at a lower cost than a separate research aircraft. The IAGOS-CARIBIC (In-service Aircraft for a Global Observing System - Civil Aircraft for the Regular Investigation of the atmosphere Based on an Instrument Container) project exemplifies the use of passenger aircraft in atmospheric observations, which has complemented satellite and ground-based data and validated models for over a decade (Petzold et al., 2015).

However, while such campaigns are great for utilising sophisticated equipment to measure the upper atmosphere during international flights, a different approach is required to investigate specifically the vertical aerosol profile. Smaller, light aircraft cover less horizontal distance and climb at slower speeds, so can achieve a better measurement resolution in the lower atmosphere. Instruments still need to be compatible with fast altitude changes and high airspeed, and ideally an isokinetic sampling inlet would be used. An isokinetic inlet ensures the air enters the sampling nozzle with the same velocity as it is moving in undistributed air, thereby preventing a skewed measurement which can occur if the sample velocity is too slow. Drawbacks of using aircraft for vertical profile measurements include the still relatively high costs, inability to adequately sample the lowermost atmosphere due to safety, and that combustion engine planes are a source of aerosol particles themselves and thus their exhaust plumes may affect measurements (Villa et al., 2016; Mamali et al., 2018).

2.2.2 Unmanned aerial vehicles in aerosol measurements

Although published results of vertical profile measurements performed with UAVs have been increasing in the last few years (Villa et al., 2016), this is still a relatively new and quickly advancing technology which couples well with the ongoing evolution of portable aerosol instruments. The main benefits of using UAVs for aerosol measurements are the relatively low costs and high versatility (Villa et al., 2016; Hedworth et al., 2021). Unmanned aircraft can be roughly separated into two main groups, fixed wing and multi-rotor UAVs, but the range of device shape, size, payload capacity, and battery life is vast. Fixed-wing drones are typically capable of longer flight time and carrying heavier loads, but have less flexibility in takeoff, landing, and flight strategy. Drones with rotors have the ability to hover in one location, which can help to stabilise the flow of aerosol sensors and minimise effects of pressure changes. This additionally makes them a valuable tool for highly accurate plume measurements. However, the placement of the sensors and/or inlet must be carefully considered to minimise the effects of the rotor downwash (Hedworth et al., 2021; Haugen et al., 2022). Generally the larger the UAV, the more it can carry but the less time it can spend in the air. Cold temperatures and high wind speeds can also further deplete battery life. The suitability of drones in vertical profiling is therefore also closely linked to the suitability of the aerosol sensors which can be deployed on the platform. Aside from technical limitations, UAV-regulations can be quite restricting and permits are typically required to fly higher than the standard 120 m roof (EU and many other countries). Attempts to integrate UAVs into managed airspace with so-called 'U-space' has begun in the EU, with the goal of facilitating further research and development of UAV technology and applications.

Chapter 3

Method

3.1 Vertical profiling measurement locations

The UAV-based vertical profile measurements were performed at the combined ACTRIS (Aerosol, Clouds and Trace Gases Research Infrastructure) and ICOS (Integrated Carbon Observation System) research station Hyltemossa, in southern Sweden (56°05'52.2"N 13°25'12.4"E). The area is classified as a humid temperate climate with mild summers and winters, and the site is located in a managed spruce forest with a tree height of around 20 m. The site was chosen due to ACTRIS reference instruments monitoring near-ground aerosol concentrations which could be used as reference for the drone-based measurements. The UAV was launched from two locations, at the main research station, and at the new ACTRIS building, as shown in Figure 1. At the main research station, there is a 150 m high measurement tower maintained by ICOS. This counts as an obstacle according to UAV regulations, therefore the UAV could be flown 15 m above its height within a 50 m radius, meaning it could reach a total of 165 m through a small opening in the tree canopy. At the second location by the new ACTRIS building in an open marshland approximately 500 m from the main tower, the drone could only fly to a maximum of 120 m due to Swedish and EU regulations.

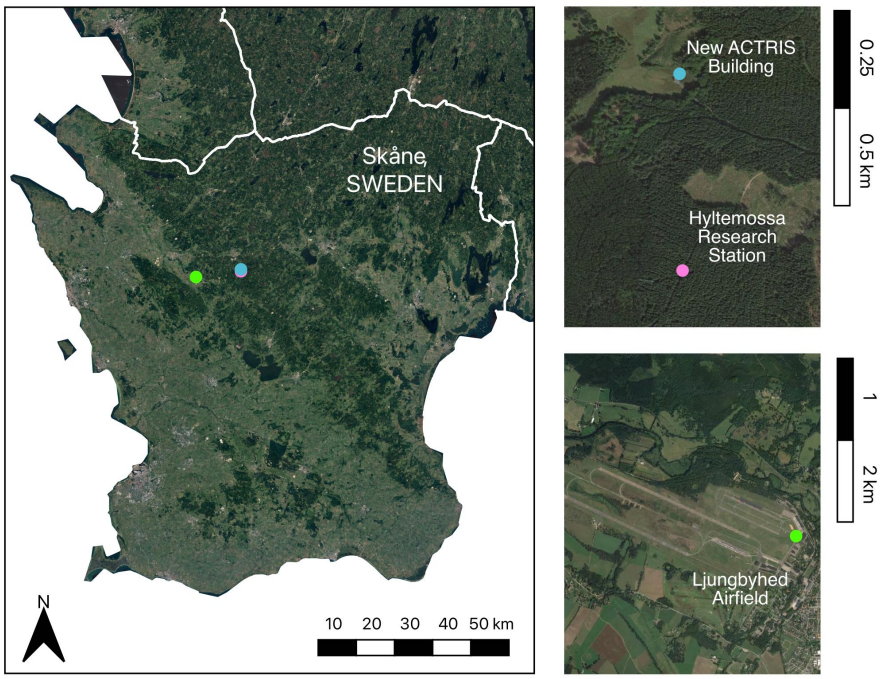

Figure 1: Map of Skåne, Sweden showing the location of drone flights at Hyltemossa and the Ljungbyhed airfield where plane-based measurements were based.

Aerosol measurements from manned instructional aircraft operated by LUSA were based at the Ljungbyhed airport (56°04'55.3"N 13°13'55.9"E), approximately 12.5 kilometers from Hyltemossa. The five plane flights had varied routes which are mapped in in Figure B.7. The Ljungbyhed airfield has been suggested as a possible future base for higher altitude UAV flights in conjunction with the LUSA drone lab.

3.2 Description of Sensors

3.2.1 Partector 2

The Partector 2 (Naneos Particle Solutions GmbH, Windisch, Switzerland) is a hand-held aerosol dosimeter (8.8 x 14.2 x 3.4 cm) weighing 415 g made for measuring nanoparticles with a high time resolution of 1 s. It is primarily designed for quantifying the lung-deposited surface area (LDSA), a metric used in health applications representing the surface area of the particles most likely to be deposited in the lungs. The instrument imparts a pulsed unipolar charge on the aerosol being drawn through the inlet with a $0.5\,\mathrm{L\,min^{-1}}$ flow rate. This leads to clouds of charged aerosol that induce a current in an electrode, the amplitude of which can be translated to the corresponding LDSA value (Fierz et al., 2014).

Along with measuring the signal for LDSA (0–12 000 $\mu\mathrm{m^2\,cm^{-3}}$), the Partector 2 measures a signal to determine the average particle diameter (in the range 10–300 nm), then from these values, calculates and reports the total number concentration (0–10^6 $\mathrm{cm^{-3}}$). Since LDSA is not particularly relevant in ambient environmental monitoring, this project primarily used the measurement of number concentration. The instrument is calibrated for a lognormal PSD, thus uncertainty in the reported number concentration arises due to the unknown shape of the distribution in the measuring environment. Internal temperature and relative humidity (RH) plus ambient pressure are recorded, and according to the manufacturer, some internal compensations for temperature and pressure changes are applied in order to limit their effects on the aerosol measurement.

3.2.2 MA300

The microAeth MA300 (AethLabs, San Fransisco, CA, USA) is a small (16.5 x 12.5 x 4 cm), portable sensor weighing 715 g. It interprets the BC concentration in real-time (down to 1 s), based on the well-established Aethalometer measurement principle, first described by Hansen et al. (1984). Particles in an air sample are continuously deposited on a filter tape in 3 mm diameter spots. Monochromatic LED light sources illuminate the sample and a detector measures the amount of light transmitted through the filter, which is reduced by accumulated light-absorbing particles. The sample signal's intensity

is compared to a reference signal measured without particle loading to determine the optical attenuation. The change in attenuation during a time period is converted to a mass concentration of BC ($\mathrm{ng\,m^{-3}}$), using a value of optical absorbance per unit mass of BC.

In so-called DualSpot® mode, particles are collected in two spots with different flow rates and measured in parallel to be used in an algorithm compensating for the loading effect, which skews the attenuation measurement if the filter is saturated (Drinovec et al., 2015). Measurements are made over five distinct wavelengths, with the longest wavelength 880 nm (empirically determined to be most absorbed by BC) providing the measurement for BC concentration. As this is in the infrared range, AethLabs refers to measurements at this wavelength as IRBC (infrared black carbon).

The MA300's internal diaphragm pump can be set with five flow rate settings between 0.05 to $0.15\,\mathrm{L\,min^{-1}}$, with two internal mass flow meters measuring and regulating the flow of the sample air stream. Both UAV and plane-based measurements in this project utilised a flow rate of $0.15\,\mathrm{L\,min^{-1}}$, as recommended by AethLabs for measurements in areas of low BC concentrations and when using DualSpot® loading compensation. Of the available timebase settings, 10 s was used in drone-based measurements which required rapid data collection, despite the higher noise (low signal-to-noise-ratio) associated with faster timebases. For plane-based measurements, a 30 s period was used as recommended for ambient monitoring applications, while still being short enough to capture changes during fast ascents and descents. Sample temperature and RH, as well as internal temperature and pressure are recorded by the MA300.

3.2.3 OPC-N3

The OPC-N3 (Optical Particle Counter) by Alphasense (Essex, UK) uses optics to detect, size, and count particulate matter in the size range 0.35–40 µm. The sensor is only 7 x 6 x 6.4 cm and weighs less than 105 g. At a price of around €300 per unit, it is classed as a low-cost sensor and the cheapest of all instruments used in this study (the other instruments cost upwards of €10 000). Particles are drawn into the sensor through an inlet with the help of a small motorised fan, where they pass through the beam of a diode laser with a wavelength of 658 nm. Individual particles scatter the light towards an elliptical mirror that reflects the light to a detector and when the amount of scattered light is converted to an electrical signal the particle's size can be determined based on previous calibration signals. Polystyrene Spherical Latex (PSL) particles with known diameter and refractive index (RI) are used in calibration since these properties allow the scattering to be predicted with Mie theory. All particles are represented with a spherical equivalent size regardless of their shape.

The OPC-N3 sorts and counts particles into 24 bins according to their size, and this

histogram data is then automatically used to calculate the mass of particulate matter per unit volume of air ($\mu g\,m^{-3}$) for PM1, PM2.5 and PM10 (i.e. the mass concentration of particles with diameter of 1, 2.5, or 10 microns or less). Histograms along with the rest of the data can be recorded in intervals of approximately 1.4 seconds. The calculation of the mass fractions assumes a default particle density of $1.65\,g\,cm^{-3}$ and RI of 1.5. Alphasense states the OPC-N3 is suitable for use in environments with up PM2.5 concentration to $2000\,\mu g\,m^{-3}$, with a maximum possible particle count rate of 10 000 particles per second.

Due to the use of a small fan rather than a pump, the OPC-N3 is very sensitive to pressure drops and thus cannot be used with sampling inlets. The sample flow rate (SFR) is documented as typically $0.28\,L\,min^{-1}$, although there is no flow meter in the sensor and external flow meters create too large of a pressure drop to measure this. According to the manufacturer, the SFR is measured with a time of flight method, whereby the time it takes particles of certain sizes to pass through the laser is related to the flow rate of the sample. The SFR value is used in calculations of PM values, and while internal sensors record the temperature and RH these values are not used in any internal calculations.

3.2.4 Aerosol Spectrometer Model 11-D

The portable (28.2 x 12.4 x 6.7 cm) Aerosol Spectrometer Model 11-D (GRIMM Aerosol Technik Ainring GmbH Co. KG, Ainring, Germany) measures the size distribution with the principle of scattered light from individual particles, similar to the less-expensive OPC-N3. The sample air is aerodynamically focused to pass through the beam of a laser diode, with a volumetric flow rate of $1.2\,L\,min^{-1}$. Each particle scatters light depending on its size, and this is detected as an electrical signal by a receiver diode perpendicular to the laser beam, allowing the particles to be counted and classified into 31 size channels between 0.25–35 µm. From the measured number and size distribution, dust mass fractions are calculated based on calibration using PSL particles and using variable particle densities. The maximum mass concentration is $100\,000\,\mu g\,m^{-3}$, and the maximum number concentration is 3 000 000 particles per liter. With a weight of 1.93 kg, the 11-D was not suitable for use alongside the other sensors on the UAV used in this project and thus only used on the aircraft.

3.2.5 SKH1 and SKS1

A modular sensor system for UAV applications (Sparvio, Sparv Embedded, Linköping, Sweden) was used as an additional measurement of environmental variables. The sensor hub (SKHI) recording temperature, pressure, RH, GPS coordinates, and barometric altitude, along with an extra environmental sensor module (SKS1) for temperature and RH were installed on the top of the drone.

3.2.6 Auxiliary measurements at Hyltemossa and Hallahus

At Hyltemossa, the aerosol above the forest canopy was sampled through an inlet on the 30 m high ACTRIS tower. The two aerosol instruments used for reference were a custom-made dual Mobility Particle Size Spectrometer (MPSS) (Leibniz Institute for Tropospheric Research (TROPOS), Leipzig, Germany), and an Aethalometer (AE33, Magee Scientific, Berkeley, CA, USA).

The MPSS measures the total number concentration in the diameter range around 3–840 nm. This instrument sorts the particles based on their electrical mobility with a differential mobility analyser and then uses a condensation particle counter to count them. The AE33 measures the BC concentration using the same principle as described for the portable MA300, also using a wavelength of 880 nm and utilising DualSpot® technology. It has a sensitivity of approximately $0.03\,\mu g\,m^{-3}$ with a 1 min timebase and $5\,L\,min^{-1}$ sample flow rate.

PM2.5 values were obtained from the aerosol spectrometer Fidas 200 (Palas GmbH, Karlsruhe, Germany). This reference instrument is located about 18 km southwest of the Hyltemossa station, at another regional background monitoring site named Hallahus (56°02'32.7"N 13°08'54.4"E). Similar to the OPC-N3 and 11-D, the Fidas 200 counts single aerosol particles and particle size fractions. The range of particle sizes measured is 0.18–18 µm, with a resolution of $0.1\,\mu g\,m^{-3}$.

Data from a ceilometer (CL51, Vaisala, Vanda, Finland) at Hyltemossa was also used to compare estimates of the BLH. This instrument uses vertical diode LiDAR pulses to measures the height of up to three cloud layers within a measurement range of 0–13 km, based on the received backscattered signal from cloud droplets and atmospheric aerosol particles. The instrument assumes particles are homogeneously distributed in the PBL and that the concentration significantly decreases above the layer and therefore, a minima in the vertical backscatter profile is interpreted as the BLH. Three candidates are given, since other minima can be be present indicating other layers in the atmosphere.

3.2.7 Summary of aerosol sensors

Table 1 includes a summary of the key features and settings of the four portable aerosol sensors.

Table 1: Summary of key features of the portable aerosol sensors and the settings used in this project.

Instrument	**Metric**	**Measurement principle**	**Diameter range**	**Time resolution (s)**	**Flow rate** ($\mathrm{L\,min^{-1}}$)	**Reference instrument**	**Platform**
Partector 2	Total number concentration	Induced current	10–300 nm	1	0.5	MPSS	UAV & plane
MA300	BC mass concentration	Attenuation (Aethalometer)	–	10 (UAV) 30 (plane)	0.15	AE33	UAV & plane
OPC-N3	PM2.5 mass concentration	Light scattering (OPC)	0.25–35 µm	1.4	0.28*	Fidas 200	UAV & plane
11-D	PM2.5 mass concentration & particle number size distribution	Light scattering (OPC)	0.35–40 µm	30	1.2	–	Plane

3.3 UAV-based measurements

The UAV used in this project was a commercial multi-copter drone from DJI (Shenzen, China), the Matrice 300 RTK. With the arms unfolded its dimensions are 81 x 67 x 43 cm, and with the two batteries included (DJI TB60) it has a weight of approximately 6.3 kg. The maximum flight time ranges from 55 min (no payload) to 31 min (with a maximum payload of 2.7 kg), however this can also be limited by wind speed (maximum wind resistance of $15\,\mathrm{m\,s^{-1}}$) and temperature (operating range is -20–50°C).

The OPC-N3 with an external battery pack and the SKHI hub and SKS1 module were mounted to the top of the drone. The payload mounted to the underside of the drone was a box containing the Partector 2 and the MA300 which were cushioned with foam and connected to a common stainless steel inlet. The inlet was 95 cm in total, with 70 cm of it extending outside the sensor box to sample air from outside the direct rotor downwash, and the remainder fed through the box for stability. This configuration of the drone and sensors is shown in Figure 2), and more pictures of the set-up can be found in Figure A.1.

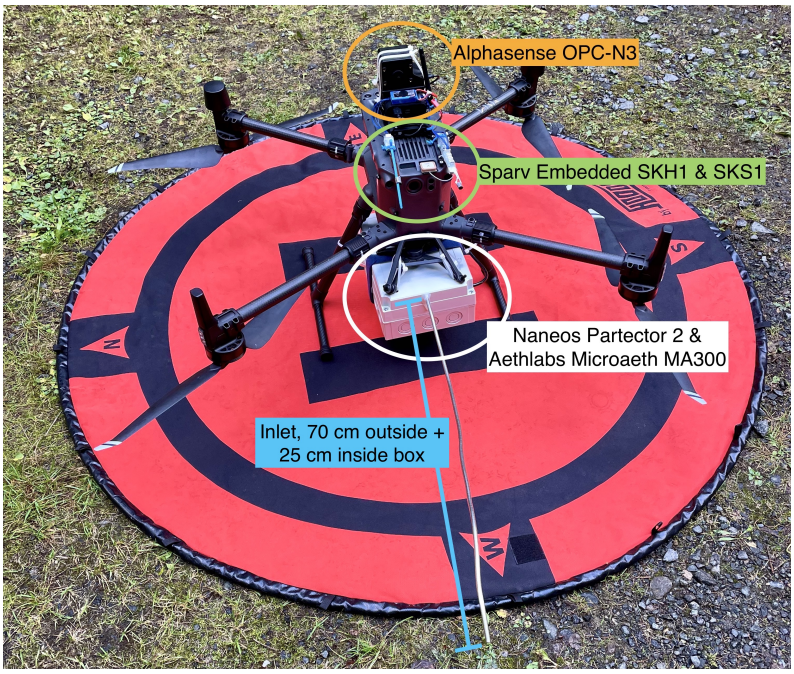

Figure 2: DJI Matrice 300 RTK on its landing pad with the sensors and inlet marked.

3.3.1 Preliminary study

This project followed on from an initial test on the 18th June 2021 by the Lund University aerosol group in collaboration with LUSA. The same drone and payload were used as described in the method above, and three flights were performed up to a maximum height of 150 m. The first flight involved a steady ascent and descent, the second included

hovering at 50, 100 and 150 m for 5 min each and descending quickly. Thirdly, the UAV ascended incrementally and hovered for around 1 min at each 10 m step. In order to decide on the flight strategy for this thesis project, the resulting vertical profiles (presented in 4) were analysed and compared to literature.

3.3.2 New measurements

For the measurements within this thesis project over the 10–11th October 2022, the UAV was again piloted by qualified persons from LUSA. During ascent, the drone stopped at altitude increments of 10 or 15 m and hovered for 2 min to increase the stability of measurements. If a change of batteries was required, the drone descended and ascended back to the next altitude step as quickly as was deemed appropriate by the operator. The descent from the maximum altitude was achieved similarly, without any particular strategy as the data collection was focused on the hovering stages. This flight strategy is exemplified in the altitude time series from the fourth vertical profile (VP #4) shown in Figure 3. Altitude time series for all seven drone flights are found in Figure B.7.

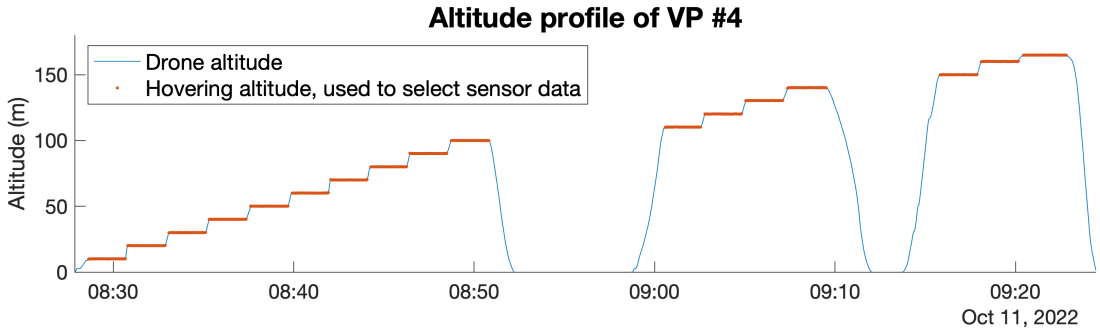

Figure 3: Example altitude profile from the fourth drone flight showing the hovering steps used in selecting the corresponding data from the sensors.

To investigate whether the forest canopy has any noticeable effect on the aerosol vertical profile, measurements at the 'tower' (close to the 150 m measurement tower) were followed as soon as possible by a measurement at the 'hut' (the new ACTRIS building). Table 2 contains the location, time and date, maximum altitude and altitude steps of the seven drone-based vertical profiles performed. Note that the time period also includes the time spent changing batteries rather than the actual flight time per battery set.

Table 2: Details of drone flights used in aerosol measurements.

VP #	Location	Time & Date	Max. alt. (m)	Alt. steps (m)
1	Tower	15:38–16:18, 2022/10/10	165	15
2	Hut	16:46–17:14, 2022/10/10	120	10
3	Tower	18:06–18:26, 2022/10/10	120[a]	15
4	Tower	08:27–09:24, 2022/10/11	165	10[b]
5	Hut	10:29–11:04, 2022/10/11	120	10
6	Tower	13:01–13:54, 2022/10/11	165	10[b]
7	Hut	15:46–16:21, 2022/10/11	120	10

[a] The maximum height of the third vertical profile had to be reduced from 165 m to 120 m due to high wind speeds compromising the safety of the flight.

[b] Since a full profile of 15–165 m was, in the end, not possible without a battery change, the altitude steps on the second day of measurements were changed to 10 m at the tower as well. An extra step of 5 m was added to complete the ascent to 165 m.

3.4 Aircraft-based measurements

During two days in May 2022 (23rd and 24th) and two days in October 2022 (13th and 19th) the aerosol sensors were placed on board various planes flown by pilot students and instructors from LUSA. The aircraft model was Cirrus SR-20, 4-seater piston-engined light aircraft with unpressurised cabins (Figure A.2). Outlets on the interior panel provide the cabin with fresh outside air which enters via an inlet at the front of the wing (see Figure A.4). This is where the Partector 2, MA300, and 11-D were set up to sample from. A common inlet connected the sensors and a silica diffusion dryer was placed in line between the cabin outlet and sensors. This set up is visible in Figure A.3. Since the OPC-N3 is not able to be connected to an inlet, it was simply placed inside the cabin to sample the ambient air. The altitude and GPS coordinates of each plane during the measurements were obtained from FlightRadar24 (www.flightradar24.com). As these plane flights were planned according to LUSA's teaching curriculum, the routes and flight strategies were not planned specifically for this project. The date, time, and some details of the flights are shown below in table 3 and maps of the plane's route are shown in Figure B.7.

Table 3: Details of plane flights used in aerosol measurements.

Flight #	Time & date	Max. alt. (m)	Route description
1	14:37–15:29, 2022/05/23	1387	Towards Helsingborg, several fast ascents/descents, looping back
2	11:43–12:16, 2022/05/24	335	Within ∼10 km of Ljungbyhed, a lot of looping around
3	09:17–10:28, 2022/10/13	2758	Ljungbyhed to Jönköping (about 220 km straight line distance)
4	12:01–13:43, 2022/10/13	2141	Jönköping to Ljungbyhed
5	19:02–20:58, 2022/10/19	822	Multiple ascents/descents at Ängelholm and Malmö airports, again at Ljungbyhed before landing

3.5 Post-processing of data

Processing and analysis of the drone and sensor data was performed in MATLAB (R2022a). All times were converted to Swedish summer time (UTC +2). Outliers in the data were assessed and removed manually.

Due to unexplained abnormalities in the attenuation values in channel 1 ('IRBC1') of the MA300 — the spot with higher flow, and equal to the BC concentration when the loading parameter is zero — during the second day of UAV measurements, the values measured with channel 2 ('IRBC2') were used for both the 10th and 11th October. This problem was not present during the plane flights, therefore the values logged as 'IRBCc' (with the loading effect compensation) are presented for that section of the results.

The values and use of standard or normal temperature and pressure conversions was found to be inconsistent amongst published aerosol vertical profile data. An attempt was made to convert measurements to standard temperature and pressure (STP) using 273.15 °K and 1000 hPa (the International Union of Pure and Applied Chemistry definition since 1982) (examples shown in Figure B.6 and Figure B.8), but ultimately this was not used in the results. Instead, the effects of changing temperature and pressure while sampling aerosols in the vertical profile was explored in the discussion chapter.

3.6 HYSPLIT trajectories

Back-trajectories were obtained from the Hybrid Single-Particle Lagrangian Integrated Trajectory Model (HYSPLIT), which simulates the origin of air masses at specified locations, times, and altitudes (Stein et al., 2015; Rolph et al., 2017). The meteorological

data input to HYSPLIT came from the Global Forecast System with a resolution of 0.25 degrees. A new trajectory was calculated for each hour during the time of UAV measurements at Hyltemossa, with a duration of 72 hr and final height of 120 m above ground level. For the plane measurements, at least 3 trajectories were obtained for each flight, one each during the ascent, cruising, and descent. The GPS latitude and longitude and altitude of the plane were used as inputs for generating the back-trajectory of the air mass at that time.

Chapter 4

Results

4.1 Preliminary study

Values of the total number, BC mass, and PM2.5 mass concentration measured each minute during the preliminary study are presented in Figure 4.

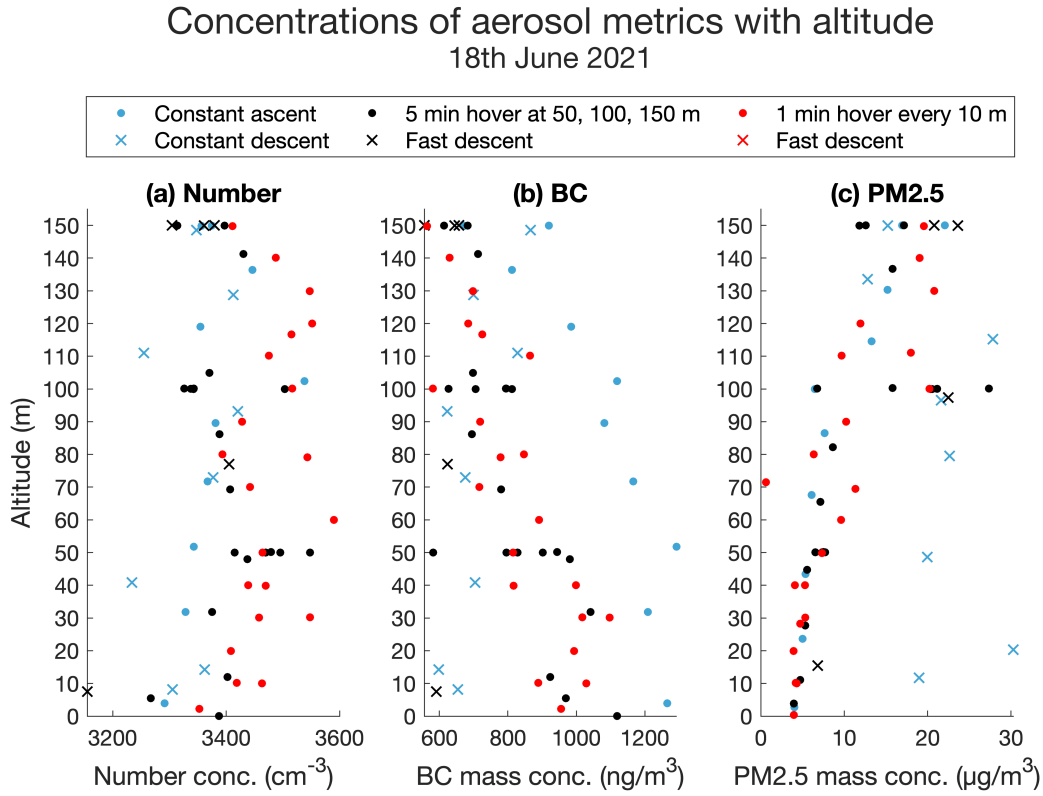

Figure 4: (a) Total number concentration (averaged from 1 s data), (b) BC mass concentration, and (c) PM2.5 mass concentration measured during the three test vertical profiles on June 18, 2021.

When the drone was piloted with a constant climb and descent, both the MA300 and OPC-N3 recorded quite differently with increasing and decreasing altitude. In accordance with other studies (e.g. Kwak et al. (2020) and Brus et al. (2021)), it was decided that only the measurements from the ascending portion was to be used in future flights. Additionally, the approach of hovering at incremental steps (also used in e.g. Haugen et al. (2022) and Alvarado et al. (2017)) was considered useful in order to help stabilise measurements in case pressure changes affect the functioning of the sensors' pumps (or fan in the case of the OPC-N3). A compromise between the hovering time and vertical resolution was reached for the new flights: hover for 2 min at increments of 10 or 15 m. In conjunction, the time resolution of the MA300 and OPC-N3 were increased to 10 and 1 s respectively to collect more data points at each altitude step.

4.2 Comparison with reference instruments

The data from the portable sensors was compared to the auxiliary measurements at Hyltemossa and nearby Hallahus with time series in Figures 5–8 below. Firstly, the entire volume of data from the portable sensors (i.e. including measurements on the ground, onboard the UAV, and while being transported by car between locations) was plotted with the corresponding stationary instruments' data from 14:00 on the 10th October to 16:30 on the 11th (Figure 5). The portable sensors mostly measured continuously throughout the day for efficiency, as turning them off between UAV flights would have required time to demount and re-mount the sensors. The benefit of including this data between flights in an initial analysis is to give an indication of whether or not the handling of equipment or changing conditions influences the subsequent vertical profiles. No data was collected by the portable sensors over night as they needed to be charged inside, where the aerosol concentrations would have differed notably from the outdoor air measured by the reference sensors.

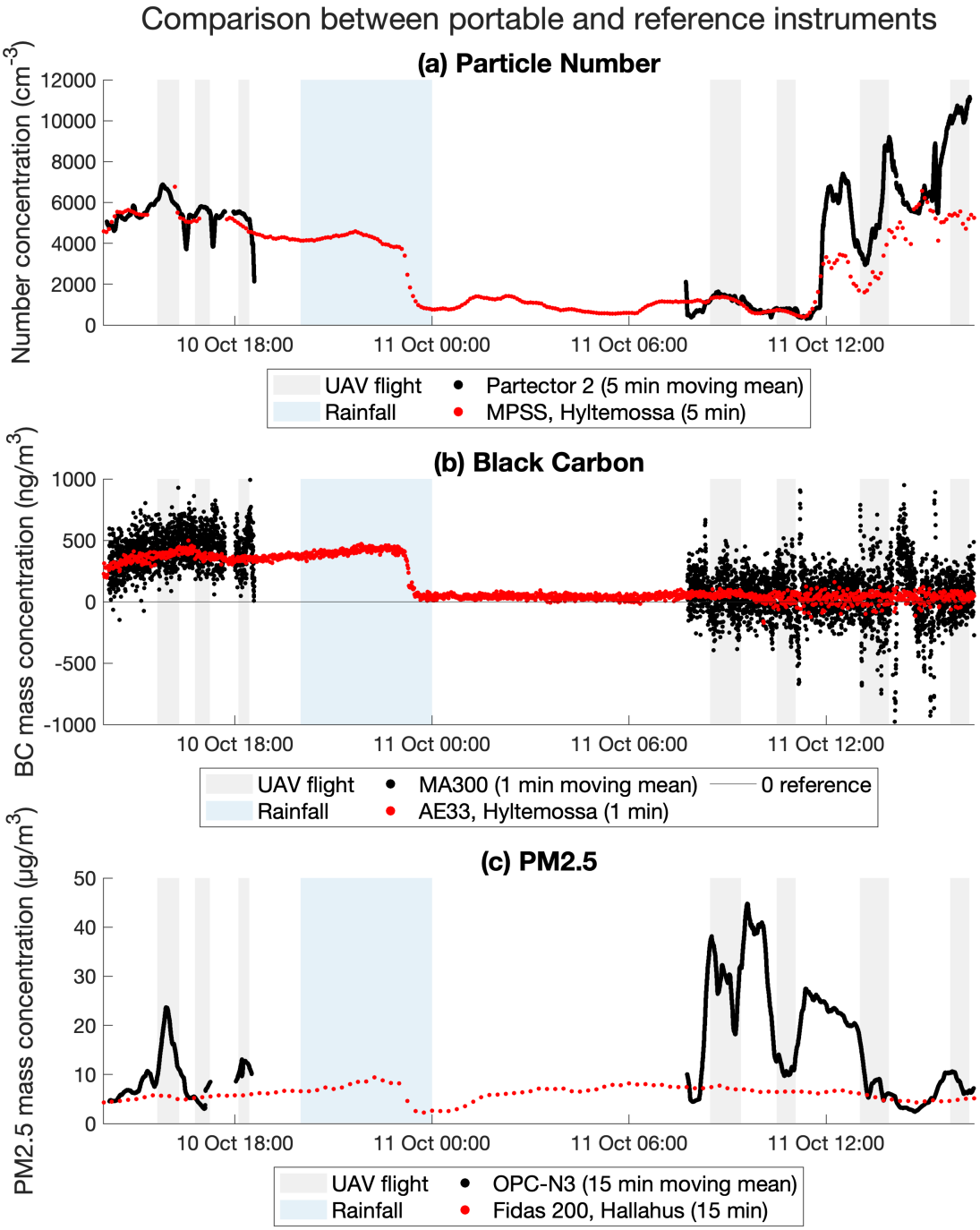

Figure 5: Time series of reference instruments from Hyltemossa and Hallahus with the full data set of each portable sensor, presented with a moving mean corresponding to the time resolution of the reference instrument.

The total particle number concentration measured by the Partector 2 appeared to follow the trends measured by the MPSS quite well, especially during the 10th October and the morning of the 11th (Figure 5a). Around 12:00 on the second day, both instruments recorded a sharp increase in number concentration, after which the Partector 2 concentration values remained generally higher. Particularly during the last UAV flight, there was a large difference between the sensors. It is also worth noting the relatively large increase

in particle number concentration measured by both instruments during the penultimate UAV flight. This highlighted the potential risk of incorrectly attributing vertical trends to altitude, when in reality the concentration also changes at the ground.

During the first day of measurements, both the MA300 and AE33 recorded BC concentrations around 200–500 $\mathrm{ng\,m^{-3}}$. During the night between measurement days, a rather sudden drop in the concentration of all metrics measured by the stationary instruments occurred shortly before midnight and was likely a result of the rainfall which occurred that evening. After this, the AE33 recorded very low, sometimes negative, BC values throughout the second day (Figure 5b). The MA300 data was also noisy around zero and contained negative values during the same period. The negative BC values arose due to the instruments' measurement principle and calculations, particularly when concentrations dropped from high to low. Although physical values inherently cannot be below zero, they can still contain valid information. The inclusion of negative values is further justified in the discussion chapter. Additional noisiness in the MA300 data was caused by the lower flow used in calculating IRBC2, which had to be used due to problems with the higher-flow IRBC1. Nonetheless, values from the AE33 were roughly central throughout the MA300 measurements.

Compared to the other two metrics, the PM2.5 time series contained more periods in which the reference instrument data (Fidas 200) was not within the range of measurements from the portable sensor (OPC-N3) (Figure 5c). The periods when the sensors onboard the UAV were in the air are shaded for reference, and the best agreement between instruments occurred during the second and second-last flights. The biggest difference was during the first flight on the 11th October, when the OPC-N3 measured around 30 $\mathrm{\mu g\,m^{-3}}$, while the Fidas 200 recorded less than a third of that value.

Three periods within the measurements in Figure 5 were chosen for closer comparison. In Figures 6–8 they are presented for (a) when the sensors were placed on the ground with the drone off, (b) while the drone hovered at 30 m altitude, i.e. the height of the aerosol sampling inlet at Hyltemossa, and (c) on the second day, again with the sensors on the ground and drone off.

The 5 min averages of number concentrations measured by the Partector 2 were within close range of the 5 min MPSS data points during the first ground and hovering comparisons in Figure 6a and b. In both cases, the one-way analysis of variance (ANOVA) tests confirmed the null hypothesis that there was no difference in means, with p-values[1]

[1]The p-value is the probability of the null hypothesis being true. A p-value below 0.05 rejects the null hypothesis, which in this case translate to concluding that there *was* a significant difference between the means of each set of sensor data. A p-value greater than 0.05 thus supports a lack of a difference between the mean values.

of 0.17 and 0.12 respectively. However, a significant difference (p = 0.0386) was found during the third comparison period, during which the range of total concentrations being recorded by the Partector 2 shifted sharply and overshot the MPSS values (Figure 6c).

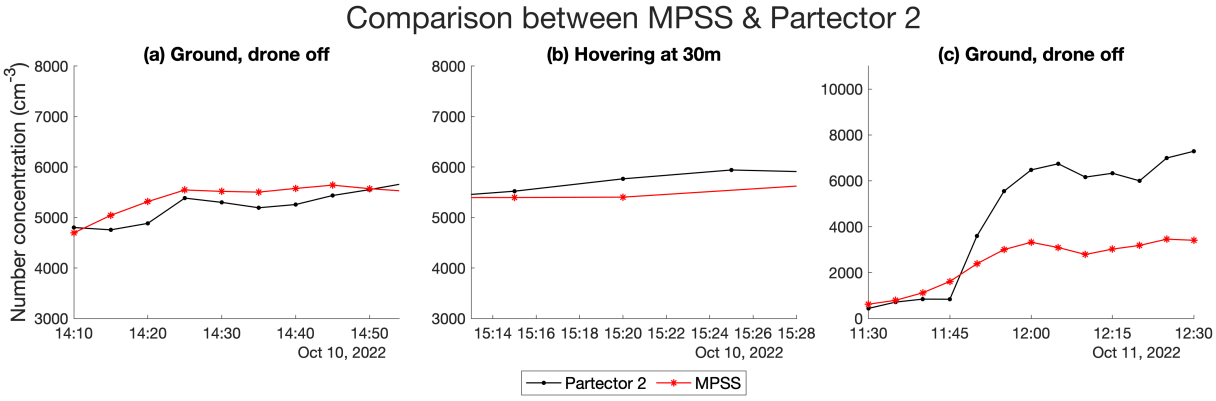

Figure 6: Time series of total number concentration measured with the Partector 2 during stationary ground measurements (drone off) and at a steady hover at 30 m and compared to the 5 min reference values from the MPSS.

The 1 min averaged BC values from the MA300 showed good agreement with the AE33 data during the three periods of comparison, and no significant difference between mean values. The p-values of the ANOVA tests were respectively 0.63, 0.25, and 0.09. During low concentrations on the 11th October, both instruments recorded more negative values.

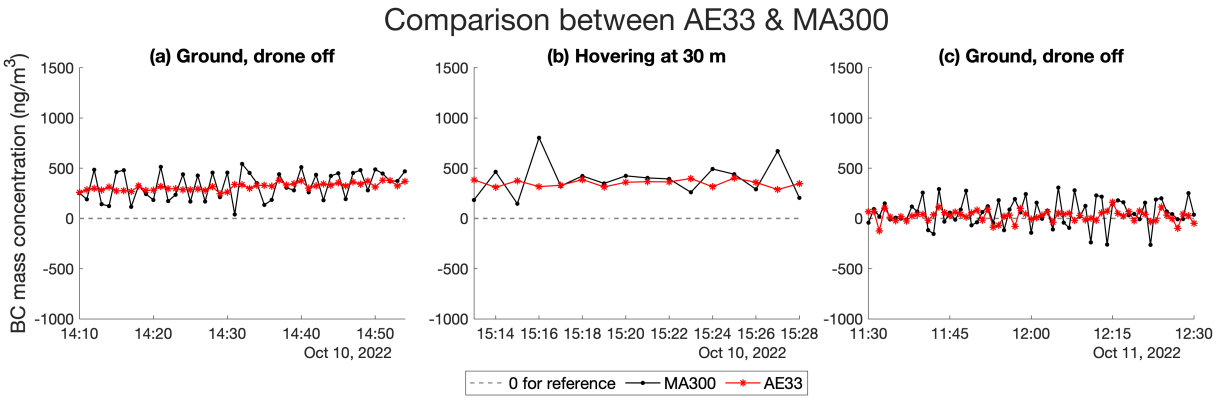

Figure 7: Time series of BC concentration during stationary ground measurements (drone off) and at a steady hover at 30 m and compared to reference values from the AE33. AE33 data given with 1 min resolution, MA300 data averaged from 10 s to 1 min.

The OPC-N3 showed better agreement with PM2.5 mass concentrations reported by the Fidas 200 during the ground comparison on the 10th (Figure 8a) than on the 11th (Figure 8). In the third comparison period, the OPC-N3 measured over twice the concentration recorded by the reference sensor, and accordingly the means of the two instruments were determined to be significantly different (p = 1.11e-07). This was not the case in the other two comparisons periods (p = 0.12 and 0.30).

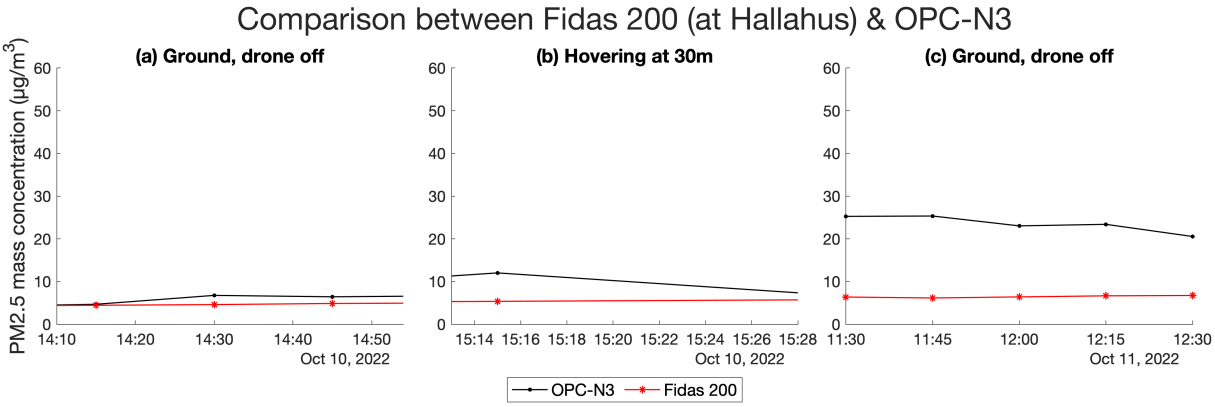

Figure 8: Time series of PM2.5 mass concentration measured with the OPC-N3 during stationary ground measurements (drone off) and at a steady hover at 30 m and compared to the 15 min reference values from the Fidas 200 at Hallahus.

4.2.1 Comparison of OPC-N3 and 11-D

During plane flights, the 11-D was used for PM2.5 profiles as it could be connected to a common inlet and drier unlike the OPC-N3, which was simply sampling cabin air from the back seat. The two instruments' data sets were compared out of interest, and the results were surprisingly quite similar even with the difference in sampling set-up (Figure 9).

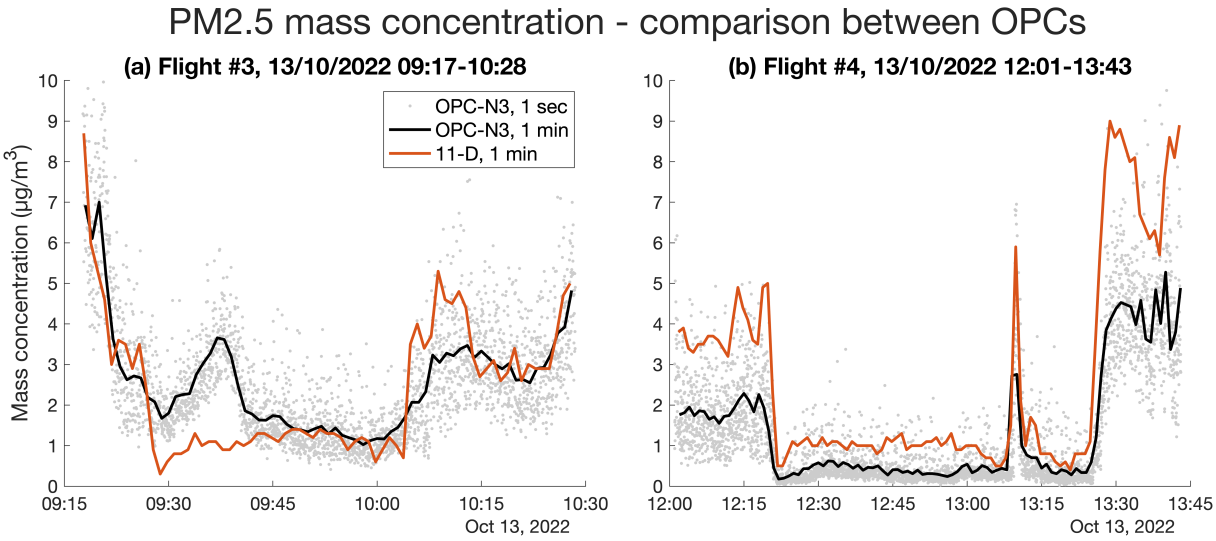

Figure 9: Comparison of the OPC-N3 and the 11-D PM2.5 measurements during plane flights #3 (a) and #4 (b).

Despite the OPC-N3 registering a peak between 09:30–09:45 which wasn't matched in the 11-D data, there was no significant difference between the two sensors' means ($p = 0.38$) during flight #3. In flight #4, the OPC-N3 consistently measured lower (in some cases half the concentration) PM2.5 concentrations than the 11-D, and a significant difference was found ($p = 7.4e\text{-}06$).

4.3 UAV vertical profiles

Figure 10 presents the results of the seven vertical profiles. Individual vertical profiles with the full spread of data during hovering stages and error bars are included in the appendix (Figure B.5).

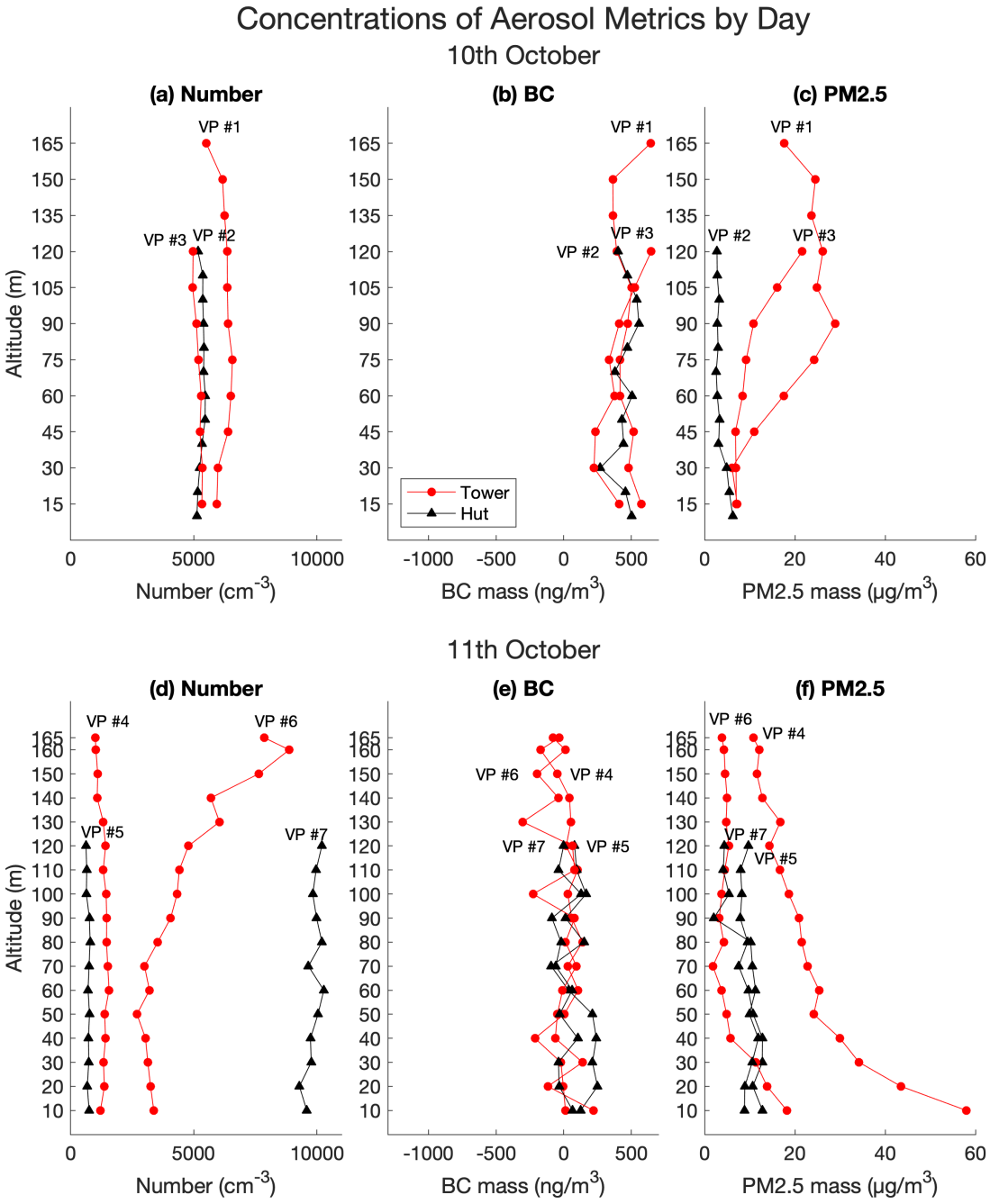

Figure 10: Vertical profiles, separated by day, of the mean particle number (a, d), black carbon mass (b, e), and PM2.5 mass concentration (c, f) during each hovering stage. The times of each flight are found in Table 2. The profiles are numbered chronologically and coloured red for measurements at the tower and black for at the hut.

VP #1–3 were measured in the space of 3 hr on the 10th October, while VP #4–7 were measured over the span of roughly 8 hr on the 11th, with between 1 to 2 hr in between. The most obvious result was the notable differences in the vertical profiles between the two days. This was supported by HYSPLIT back-trajectories visible in Figure 11, which show the varying origins of the air masses arriving at the measurement location. The higher particle number concentrations and BC mass concentrations measured on the 10th can be related to the air mass moving over Germany and Poland before arriving at Hyltemossa, whereas the lower concentrations of BC measured on the 11th were typical for a clean arctic air mass. The HYSPLIT trajectories calculated hourly during the times of measurements also show little variation in the origin and route of each day's air mass. However, there was some height variation with each hourly trajectory on day 1, and most trajectories begin at a height of around 500 m on day 2.

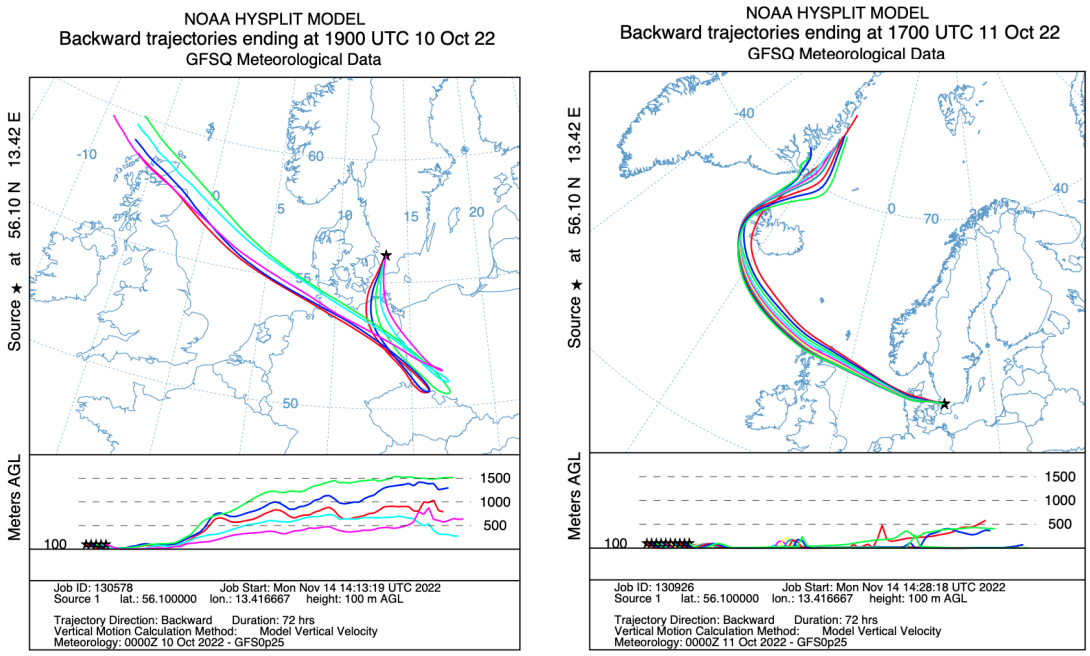

(a) 10th October **(b) 11th October**

Figure 11: HYSPLIT back-trajectories for the 72 hr prior to the air mass arriving to Hyltemossa (100 m).

The number concentration in most of the vertical profiles was relatively constant. Figure 10a shows little difference between individual profiles on the first day regardless of the location, with mean values around 5000–7000 cm^{-3}. However, while the two morning measurements on the second day were quite similar with rather low and constant values (around 650–800 cm^{-3} and 1000–1800 cm^{-3} respectively), the other two profile measurements in Figure 10d were very different. VP #6 at the tower showed a slight decrease until 50 m, but quickly increased after 70 m to almost 3 times the concentration closer to the surface. This increase was also observed in the MPSS data (Figure 6), so the increase

was not related to the altitude change. The final profile at the hut was more constant than the penultimate profile, but the values were over 10 times higher than the other profile at the hut earlier that day.

There was no distinguishable differences between the BC profiles at the tower and at the hut in Figure 10b and e. The BC mass concentrations on the 11th October were lower (below $250\,\mathrm{ng\,m^{-3}}$) compared to the previous day (around 250–$600\,\mathrm{ng\,m^{-3}}$), and several of the mean values were close to or below zero. In comparison to the vertical measurements of particle number and PM2.5, the BC measurements contained bigger differences between each mean value at the hovering step, causing more 'zig-zagging' in the profile.

The variations in mean PM2.5 mass concentrations with altitude were seemingly slightly less at the hut location (under $20\,\mathrm{\mu g\,cm^{-3}}$) than at the tower (up to $60\,\mathrm{\mu g\,cm^{-3}}$). Figure 10c shows a similar PM2.5 concentration for all three profiles up to 30 m, but from there the concentration increased for the two profiles at the tower, while VP #2 at the hut showed a slight decrease with altitude. Three of the four profiles in Figure 10f were quite similar, but VP #4 at the tower was set apart from the rest with the PM2.5 concentration up to 3 times higher at the first hovering altitude.

4.4 Aircraft-based measurements

4.4.1 Vertical profiles

Of the five plane flights, only two were deemed suitable for presenting the vertical profile during ascent and descent. The other measurement flights were complicated by the flight strategies, including frequent direction changes and repeated landings and takeoffs to low altitudes with too short ascent and descent times. Figure 12 and Figure 14 below show the resulting aerosol concentration profiles and corresponding plane altitude time series from two flights on the 13th October (flights #3 and #4). 1 min averages of (a) total number concentration from the Partector 2, (b) BC mass concentration from the MA300, and (c) PM2.5 concentration from the 11-D are presented.

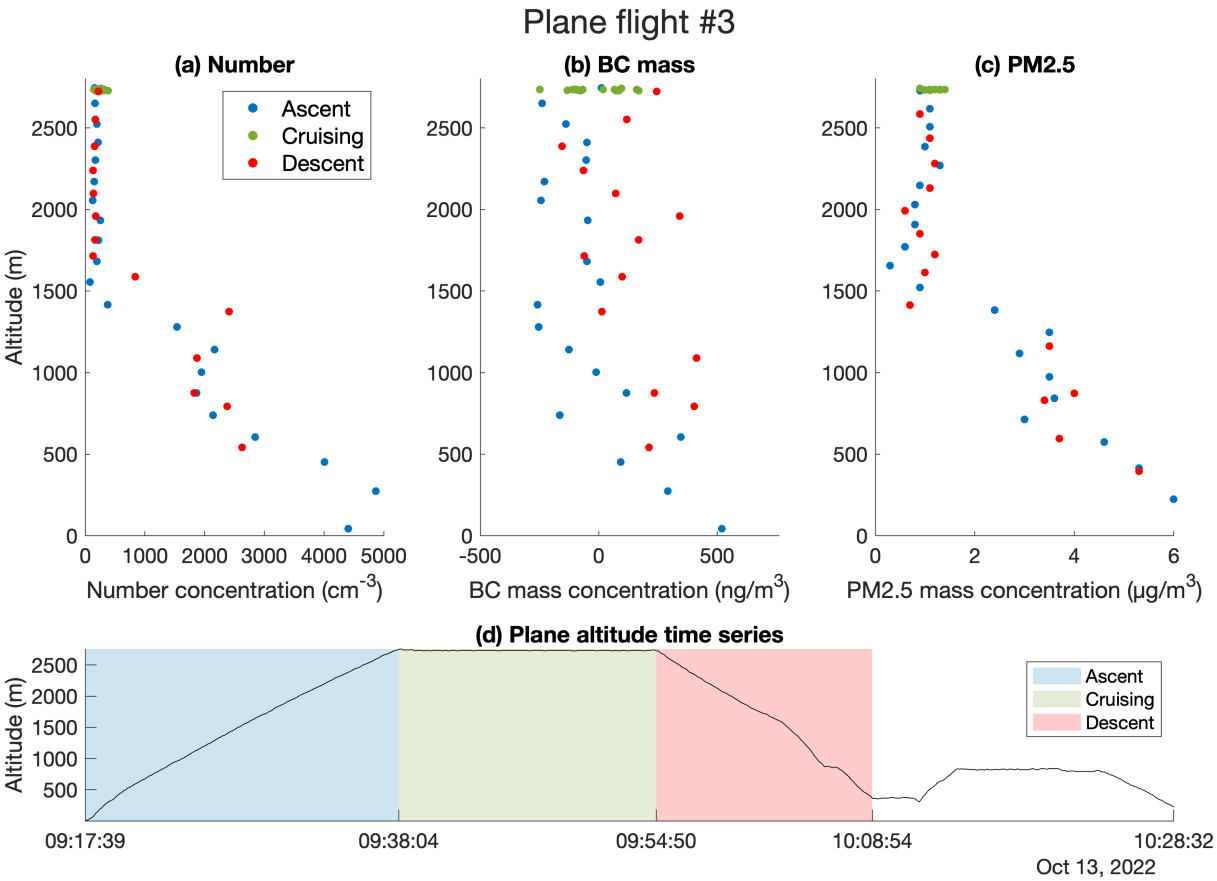

Figure 12: 1 min resolution of (a) total particle number, (b) BC mass, and (c) PM2.5 (from 11-d) concentrations with altitude during flight #3. Plane altitude over time shown in (d), with data separated into ascent, cruising, and descent.

Both the total particle number concentration (Figure 12a) and PM2.5 mass concentration (Figure 12c) decreased after takeoff up to an altitude about 1500 m. From there until the plane reached the cruising altitude of 2700 m, the concentrations were much lower and more constant. Despite the plane taking off in Ljungbyhed and landing approximately

220 km away in Jönköping, these values were followed closely upon descent as well. The BC mass concentration (Figure 12b) varied more between the ascent and descent portions of the flight, with generally lower values during ascent. Above around 1000 m the BC concentration was noisy around 0, with many negative values especially during the ascent portion. The data seemed more spread than for the other instruments which cannot record values under 0.

The last 20 min of the flight was excluded from analysis (Figure 12d) due to the flight strategy. The pilot appeared to perform a 'touch-and-go' (where the aircraft lands on the runway but immediately takes off again) before looping around and finally landing. Note that the altitude at the end of the time series was 220 m, a result of Jönköping airport's higher elevation and the plane's barometric altitude calibration.

An example of the HYSPLIT back-trajectories obtained during the flights is shown in Figure 13. During flight #3 (09:17–10:28) the air masses arriving to the plane's location/altitude at each of the chosen points at 09:00 and 10:00 were quite close. The trajectories during ascent and descent at 1000 m were similar in that they both travelled over central Europe. At the point chosen during the cruising portion of the flight, the air masses had not descended lower than 1500 m in the 72 hr they travelled over the south of the UK and across the North Sea and Denmark.

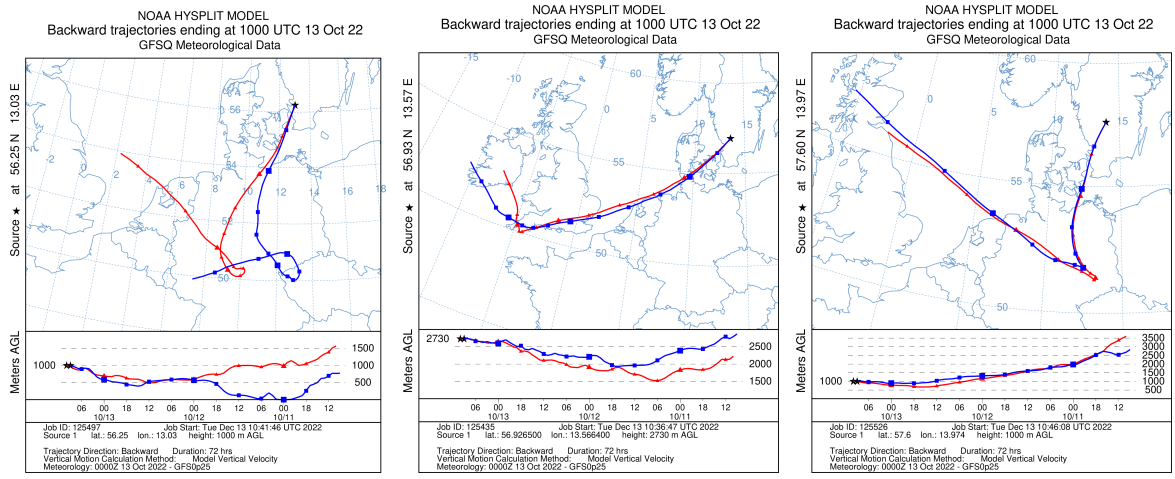

(a) Ascent **(b) Cruising** **(c) Descent**

Figure 13: HYSPLIT back-trajectories during flight #3 on the 13th October.

During flight #4, the returning flight from Jönköping to Ljungbyhed, the total number concentration again showed a decrease from ground to around 1400 m followed by constant low concentrations in ascent up to the cruising altitude of around 2100 m, and a similar trend upon descent (Figure 14a). Above around 1400 m, the BC mass concentration was again noisy around zero with negative values (Figure 14b), suggesting similarly low concentrations at the higher altitudes. The PM2.5 profile in Figure 14c similarly showed

low concentrations above 1400 m but higher values were observed during descent. During the longer cruising time of around 52 min, the data of all instruments was more spread than in flight #3 (which cruised for 16 min). The first 13 min of the flight were excluded again due to flight strategy not being ideal for vertical profiling (Figure 14d). On descent, the plane appeared to reduce its altitude in increments, which resulted in spread out clusters of data while the altitude was constant.

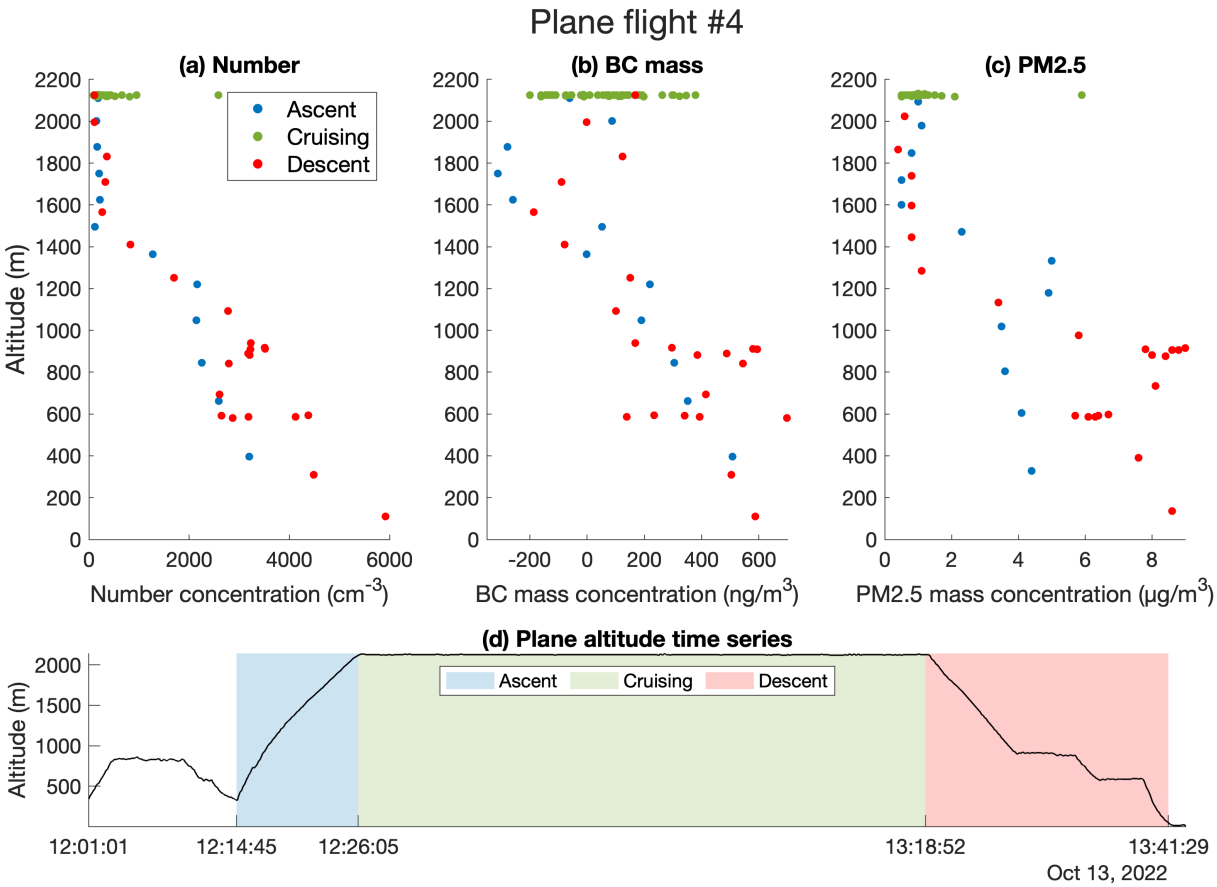

Figure 14: 1 min resolution of (a) total particle number, (b) BC mass, and (c) PM2.5 (from 11-d) concentrations with altitude during flight #4. Plane altitude over time shown in (d), with data separated into ascent (blue), cruising (green) and descent (red).

From Figures 12 and 14 above, it was suspected that the plane crossed the boundary level at around 1500 m in accordance with the drop in aerosol concentrations. The mass concentration of the 31 bins classified by the 11-D were plotted over time with the altitude overlaid in Figure 15 below, and the sharp change in aerosol was also very clear.

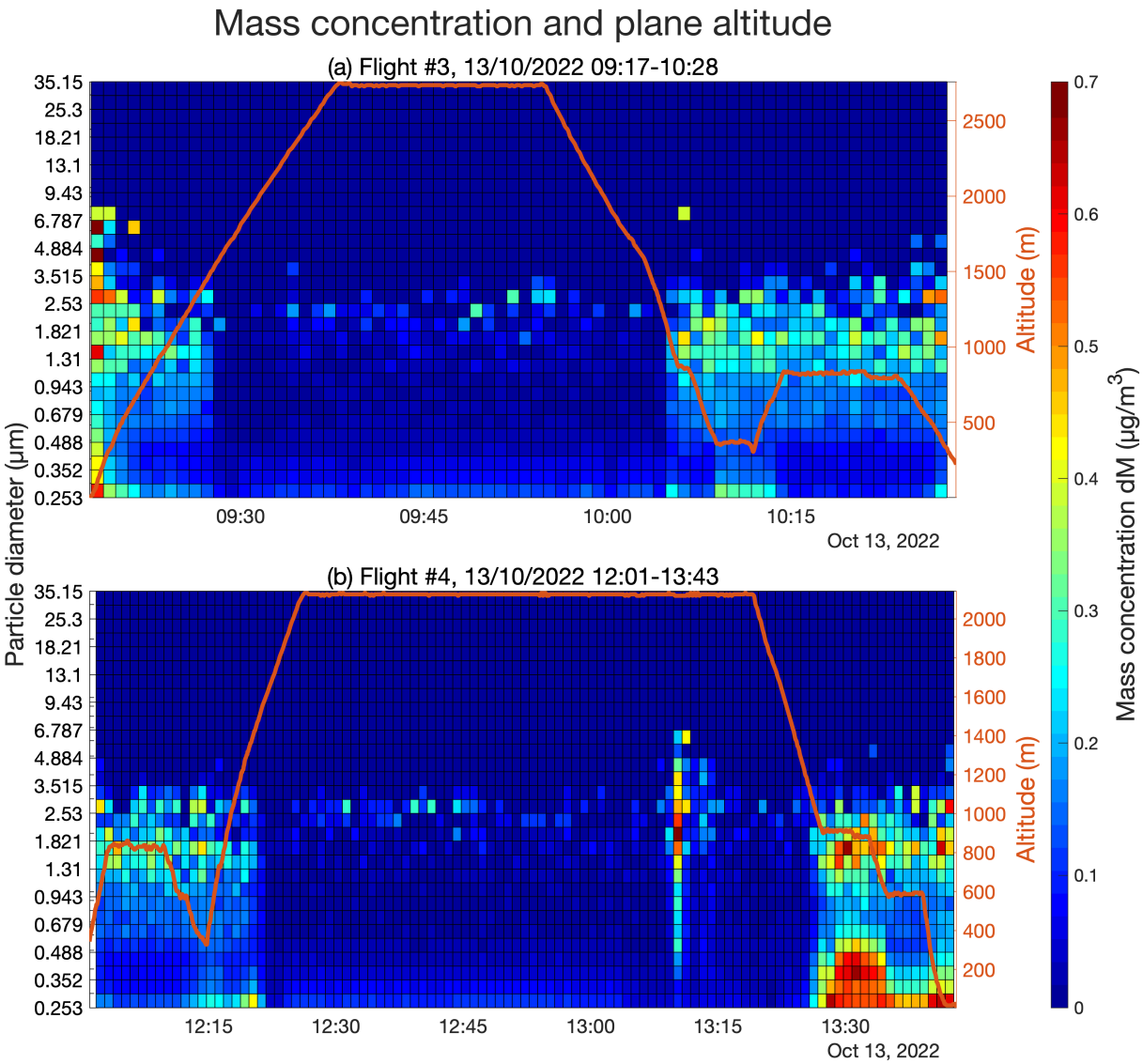

Figure 15: Mass concentrations of each of the 31 bins measured by the 11-d over the course of (a) flight #3 from Ljungbyhed to Jönköping and (b) the return trip, flight #4.

During flight #3, the concentration of all particle sizes dropped quite suddenly when the altitude reached 1500 m on ascent. The low concentrations were quite consistent until around 1250 m on descent. The same was seen during flight #4, except there was a spike in concentration across several bins around 2 µm around 13:10. This was also observed in the Partector 2 and OPC-N3 data, but could not be explained by back-trajectory analysis.

In an attempt to match these observations with the BLH during the same time, data from the CL51 at Hyltemossa is presented in Figure 16.

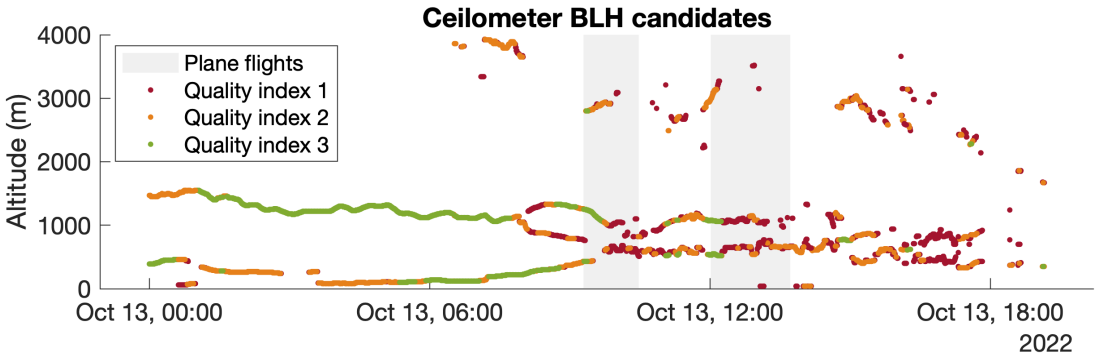

Figure 16: Boundary layer height candidates from the CL51 located at Hyltemossa.

The raw data from the CL51 includes the candidate values for the BLH coloured according to the quality index where 3 is the best. During the two flights presented above, there was a rough line around 1000 m, but also a second lower line was visible around 500 m with some scattered higher points.

Chapter 5

Discussion

5.1 Comparison of portable sensors to reference instruments

Overall, the portable sensors Partector 2, MA300, and OPC-N3 performed reasonably well in comparison to the reference instruments MPSS, AE33, and Fidas 200. The ANOVA tests showed no significant difference between the means of each instrument in 2 of 3 cases for number concentration, in all 3 for BC concentration, and in 2 of 3 cases for PM2.5 measurements. The similarity between measurements both when on the ground with no influence from the drone as well as while hovering at 30 m was indicative of two things. Firstly, that there was no distinct difference between the aerosol concentrations measured by reference instruments with a 30 m high inlet and the concentrations measured on the ground. Secondly, that the instruments were suitably mounted on the drone such that the disruption to the surrounding airflow did not affect the aerosol concentrations while hovering. An attempt to explain the two cases in which the means *were* found to be significantly different during the third comparison period follows.

The Partector 2 seemed to overestimate the total number concentration in comparison to the MPSS during the ground comparison on the 11th October (Figure 6c). The data from the MPSS had not been quality controlled, so sampling losses for particles with diameters under 10 nm were not accounted for, but this is anyway below the range of the Partector 2. Around 11:50, the 1 s raw Partector 2 data showed a clear shift in the range of number concentrations being recorded, which was found to be consistent with a reduction in the average particle diameter (Figure 17a), as well as the deposition voltage (DV) dropping from high to low (Figure B.2). In 'adaptive DV' mode, the Partector 2 measures the full range of 10–300 nm particles by switching the voltage of the internal precipitator (as opposed to only measuring 20–150 nm with a fixed voltage) when the particles are very small or very large, and this explains the discontinuity in the raw values. It could not be determined why the average diameter was reduced, but the higher number concentrations after this shift could be attributed to the calculation based on inaccurate diameter values. The Partector 2 is calibrated assuming a lognormally distributed PSD, which on a linear diameter scale translates to smaller particles being more numerous.

An interesting additional observation was that the shape of the MPSS total number concentration closely followed the trend in LDSA measured by the Partector 2 during the same time (Figure 17b). This indicates that the instrument was in fact measuring correctly, but that the error arose when using the average diameter to calculate the total

number concentration. Although the metrics are not exactly comparable, they can both be related to the total surface area of the aerosol and are thus proportional in some way.

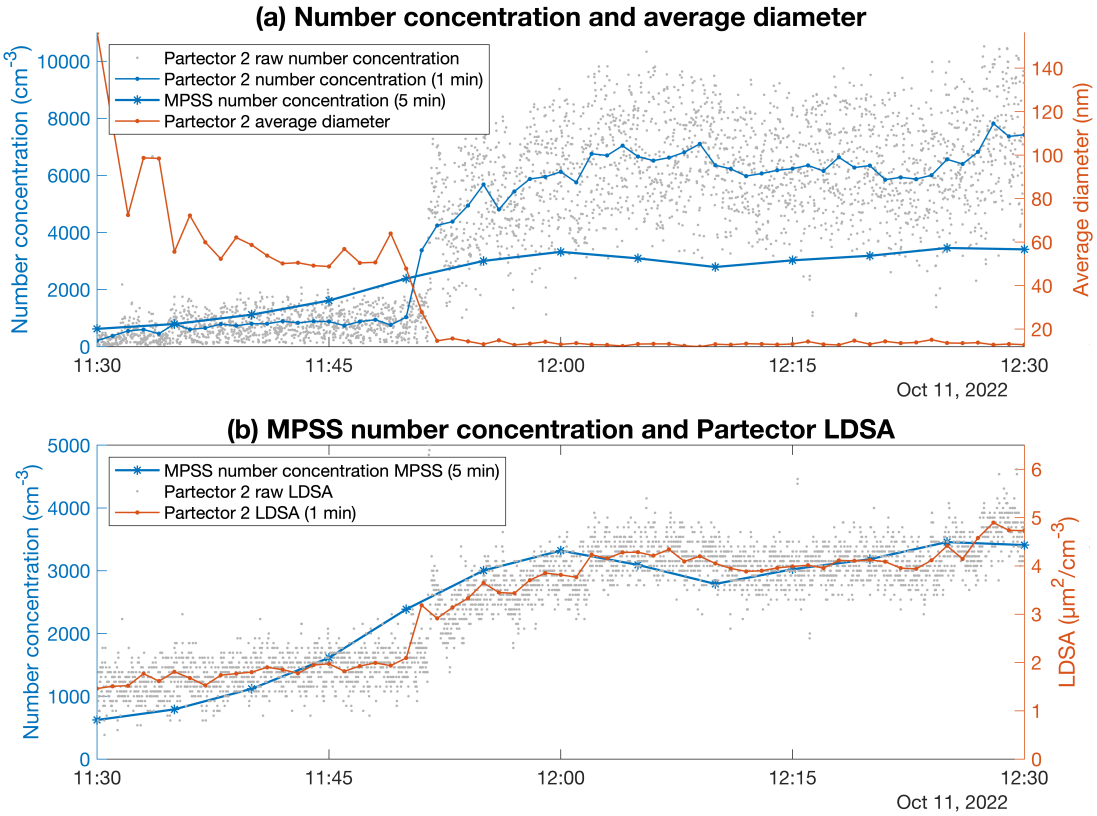

Figure 17: Number concentration, average diameter, and LDSA during the ground comparison of instruments on the 11th October.

Naneos has released an upgrade to the Partector 2 implementing an eight-channel size distribution by iterating through different deposition voltages. This may reduce some discontinuity if the voltage were to be changed in a more controlled fashion and potentially offer some improvement to the calculation of total number concentration. This data could be compared to MPSS particle number size distributions (example data shown in Figure B.3) and provide further insight into processes such as new particle formation if used in future studies of nanoparticle vertical profiles.

During the same comparison period, the OPC-N3 measured over double the PM2.5 concentration measured by the Fidas 200 reference instrument. This was believed to be a result of RH, which is known to cause problems with the low-cost OPC. Water droplets would have been retained in the trees after the overnight precipitation, thus the air close to the ground would likely have taken longer to dry than the air higher up. This could explain the higher RH conditions close to the ground as the water evaporated compared to the lower RH measured on the ICOS tower (see Figure B.4 for temperature and RH tower measurements over the two days). The OPC-N3's internally measured RH was

about 10–20% higher during the ground comparison on the second day (Figure 18), but this was probably much higher in reality, since the sensor does not accurately measure ambient RH at high values.

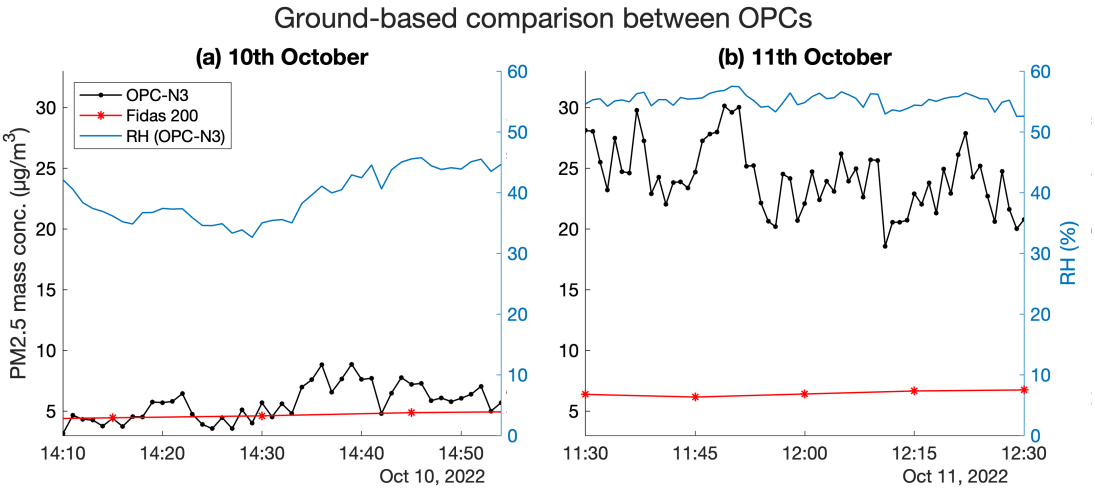

Figure 18: OPC-N3 and Fidas 200 PM2.5 concentrations during the two ground comparisons with RH measured by the low-cost sensor.

For future campaigns, these sensors should undergo longer periods of comparison with reference instruments and be calibrated or corrected as needed. The value of having ground-based instruments sampling at the same time as in-air measurements was exemplified in Figure 5a. Even if the instruments at ground level were to be other calibrated portable sensors, this could help avoid misinterpreting decreasing or increasing ambient concentrations as a function of altitude.

5.2 Vertical profiling results

In total, seven UAV-based vertical profile measurements were made over two days in October 2022, and the sensors collected data during 5 plane flights over 4 different days in May and October 2022. The resulting profiles provide confidence in the viability of these methods.

The secondary aim of investigating whether the forest around the ICOS 150 m tower and current ACTRIS 30 m tower has an effect on the aerosol vertical distribution was tested by performing vertical profiles at both the tower and hut locations. In most cases, there was little difference between the vertical concentration gradients measured at the tower and those measured at the hut. Even though the inlet length should have minimized the downwash effect during the flight, while the UAV was still close to the ground (up to around 20 m) there was considerable disturbance in the air below, which may have disrupted any vertical differences in the near-ground air. This also contributed to the decision to only use the measurements during ascent. However, since air in the 120–165 m

layer sampled in this campaign was expected to be well-mixed anyway, it is possible that the mixing beneath the UAV was not significant in comparison to atmospheric processes.

As shown in Figure 10, the main differences between vertical profiles were related to the day the measurements were performed, and thus representative of the different air masses present at Hyltemossa on each day (Figure 11). The profiles which did show some change with altitude could mostly be linked to another factor than altitude. As mentioned, the increase in number concentration observed in VP #6 was actually just a result of the measurement coinciding with the concentration increasing over time, as was visible in the ground data. The last flight resulting in VP #7 showed consistently high concentrations with altitude (around 10 000 cm^{-3}), while the MPSS measured around half these values (Figure 5a). The cause of the higher values was unclear, but might be related to the small average diameter and low DV during this period (Figure B.2), as was the case in the second comparison period (Figure 17).

Several features in the profiles may also be linked to the precipitation event which occurred overnight between measurement days. The BC concentration was much lower, and more negative and zero values were recorded. The low number concentrations in the two morning profiles (VP #4 and #5) could have been a result of particles being removed from the atmosphere by the rainfall. The seemingly decreasing PM2.5 concentration with altitude in VP #4 was likely due to the higher RH at the ground, which also increased the concentration during the second ground comparison (Figure 18b). RH may also have caused the increased PM2.5 values at higher altitudes observed in VP #1 and #3, as the measurements on the tower were around 85–90%. Aside from these cases, the majority of vertical concentration profiles were relatively constant with altitude, suggesting a well-mixed aerosol.

The higher altitude vertical profiles achieved with the sensors on board the two plane flights on the 13th October showed greater difference with altitude. The profiles were characterised by a steady reduction in number and PM2.5 concentration with altitude, and distinctly lower and more constant concentration during ascent and descent above 1500 m. The BC concentration appeared to be less constant above this altitude, but the negative values skew the profiles. This was the same in the period of low BC concentration during UAV-based measurements when the MA300 recorded noisy data around/below zero. If the BLH is defined by a sharp decrease in aerosol concentrations, it could be assumed that the PBL extended to 1500 m during these measurements. While data from the CL51 ceilometer at Hyltemossa (Figure 16) was not an exact match for this, the drop in concentration was still most likely a result of the plane entering the free troposphere. A similar profile should have been achieved with a UAV permitted to fly above the regulated 120 m, with the added benefit of slower ascent speed allowing for more data to be

collected.

5.3 Suitability of sensors in vertical profile measurements

The portable sensors Partector 2, MA300, OPC-N3, and 11-D used in UAV and aircraft vertical profile measurements were selected to measure several aerosol properties, but also because they were the sensors available for use at Lund University. There are many other small sensors which have been used in other vertical profiling campaigns, but comparison with these was outside the scope of this thesis. The suitability and limitations of the four sensors used are discussed based on this project's results, and an assessment of the more general methods involved in using a UAV and instructional aircraft platform is presented below.

Primarily designed for measuring LDSA, the Partector 2 may be more suitable in vertical profiling with a personal exposure aspect where this metric is most useful. For example, the sensor has measured LDSA from a UAV-platform in a maritime port in Greece up to 40 m (Haugen et al., 2022), and the first Partector model was used in a Helsinki street canyon up to 50 m (Kuuluvainen et al., 2018; Järvi et al., 2023). Nonetheless, the reasonable agreement with the total number concentration measured by the MPSS shows the instrument can also be used for vertical number concentrations. The main issue with this instrument was the discontinuity in measurements when the DV shifted, and the resulting higher number concentrations when the average particle diameter was low. The default 1 s data allows for very highly resolved data, which is good for use on moving platforms even if it is smoothed in post-processing.

The low BC concentrations experienced on the 11th October were not the most interesting conditions for investigating the vertical distribution of BC. Both the portable and reference instruments were measuring close to their lower limits of detection, but this at least confirmed the low and noisy MA300 values were not just a result of measurement problems. Although it is not physically reasonable to have negative BC concentrations, values less than zero can arise due measurement assumptions (e.g. that attenuation changes are solely due to light absorption by BC), possible volatility of the sample, or electrical noise. As investigated by X. Liu et al. (2021), post-processing techniques and noise-reduction algorithms are still being assessed for mobile BC measurements like this. Therefore, the data was presented in its raw form to avoid potential bias from data smoothing. However, the strange attenuation values of the IRBC1 measurements on the 11th October were unable to be adequately explained. During correspondence with Aethlabs, it was suggested that moisture might have accumulated on the filter or the filter deformed due

to pressure changes, thus affecting the attenuation and calculations. On the other hand, this problem did not arise during plane flights to much higher altitudes where the sensors experienced larger pressure changes (although a dryer was used). Including a miniature dryer in the UAV set-up would reduce this potential source of error. The manufacturers are also working on implementing additional compensation for temperature and RH in future firmware releases. Additionally, there are different data-smoothing tools available through Aethlabs which could improve the visualisation of data during low concentrations, but it was decided not to use these in this project.

High RH is also a known issue for the OPC-N3 since water droplets enhance the scattering of light and thus leads to overestimation of particle sizes. A major drawback is that this low-cost sensor cannot be connected to a drier (or inlet) without significant modification. Bezantakos, Costi, et al. (2020) modified its predecessor, the OPC-N2, with a small vacuum pump providing a constant flow rate and allow for use in sampling/pretreatment lines. Even before the modification, the OPC-N3 did perform well in laboratory tests simulating temperature and pressure conditions expected during vertical profiling (Bezantakos, Schmidt-Ott, et al., 2018). Despite this, in actual UAV applications where uncontrolled air speed and wind changes can affect the flow, the use of a small computer fan to draw in sample air is not considered ideal. The SFR recorded during drone flights was not constant, but it was not able to be determined if, or how, this affected the PM2.5 data. The OPC-N3's ability to measure at small time intervals is good for this kind of application where changes occur on a fast timescale, but the lack of time-stamping of the data can cause problems when analysing the data. While it would add some extra weight to the payload, the instrument could be connected to a micro-controller with a real-time clock, as demonstrated in Soroka (2020). A micro-controller could also facilitate an external data-logger which would aid in data integration and synchronisation, and/or enable real-time data transfer and visualisation to assist in-flight strategies (Chiliński et al., 2018).

The more robust aerosol spectrometer 11-D provided valuable contributions during aircraft measurements, but was too heavy to be used on the UAV. By connecting to the common sampling inlet with a silica dryer, potential RH issues could be minimised. The 11-D comes with an additional GPS receiver which could further benefit plane-based measurements with accurate altitude readings.

5.3.1 Environmental influences

When sampling air at changing altitudes it is important to take the changing environmental conditions into consideration. Boyle's law states that the volume of a gas sample is inversely proportional to pressure (at constant temperature), while Charles' law describes the proportionality between volume and temperature at constant pressure. Within the

troposphere, both temperature and pressure typically decrease with height. The decreasing pressure increases the volume, and the expansion of air leads to cooling. The air temperature is also influenced by other factors such as surface heating, which in turn affect the air density. Since aerosol concentrations are given in number or mass per unit volume (i.e. number or mass density), the volume should ideally be kept constant for an accurate quantification of the amount of particles and comparison between altitudes. This was found to be a challenge given instrument flows and measurement of ambient variables, as well as inconsistencies in converting measurements to STP.

Firstly, the way sensors measure and control the flow should be noted. The 11-D makes an automatic altitude correction to its volumetric flow rate based on air pressure, but does not factor in temperature changes. The MA300's internal flow meters should maintain a constant mass flow, but Aethlabs warns that changes in air density can affect the volumetric flow rate. The Partector 2 and OPC-N3 don't have internal flow sensors, but the latter estimates sample flow rate based on the time it takes certain particles to pass through the instrument. Naneos communicated that the Partector 2's (undisclosed) compensation for temperature and pressure should be sufficient within normal ambient conditions. Furthermore, they expect differences between calibration and actual particle morphology and PSD shape to have a more significant affect on the instrument's accuracy than environmental conditions. Nonetheless, regular calibration of instrument flow rates should be performed, and controlled tests of temperature and pressure changes could provide useful adjustments for these sensors when used for routine vertical profiling.

Some vertical profile studies mentioned converting data to STP, although even then multiple definitions of STP were found to be used. Furthermore, since the sensors typically report values differently to ambient conditions, there was uncertainty as to which to use in conversions (i.e. the temperature of the undisturbed air, or the temperature of the sample inside the instrument). For UAV-based measurements, temperature and pressure from the Sparv modules was used to convert the measurements from the Partector, MA300, and OPC-N3 to STP. However, the relatively minimal variations in temperature and pressure within the 165 m layer had a minimal effect (see Figure B.6). For the plane measurements, there was no common measurement of ambient temperature and pressure, so the sensors' internal values were used. Although the pressure drop was more significant at higher altitudes, the sample temperature was somewhat regulated by the air exchange system in the unpressurised cabin and again the conversion had little effect (see Figure B.8). The conversion was ultimately not used in the final results due to the small apparent influence, but also uncertainties in the internal environmental readings and a lack of consistency in converting, reporting, and even measuring temperature and pressure in other vertical profile studies.

As temperature, and additionally RH, can affect aerosol measurements the accurate measurement of these variables is valuable for potential conversion or calibration. Quantifying environmental variables is also useful for modelling. However, internal temperature sensors often report higher temperatures (and consequently lower RH) than the ambient air, due to heating from electronics. For example, Nurowska et al. (2022) found that the OPC-N3 reported a higher internal temperature and lower RH of approximately 6°C and 20% respectively when compared to a specific weather instrument. Therefore, an independent sensor designed specifically for measuring the temperature and RH of the sample air should be used. The Sparvio modules used on the UAV in this project are an example of this, although they were not able to be used in the aircraft measurements. During UAV-based measurements, the Sparvio sensors always measured the lowest temperature and highest RH, confirming the internal heating. It should also be noted that no validation of the SKHI and SKS1 temperature and RH was performed, but the manufacturer states an absolute accuracy of 0.2°C and 1.8% respectively.

5.4 Evaluation of the methods

Performing measurements with UAVs requires reaching a suitable compromise between the sensor payload and the battery time. Too much weight and the available flight time may be too short to be of use, while on the other hand, sensors that are light enough to maximise flight time may not yield accurate enough data. In this project, the maximum flight time was reduced to a little over 20 min when carrying the three aerosol sensors. The cold weather (around 10–11°C) and periods of high wind speed (up to $13\,\mathrm{m\,s^{-1}}$) likely also contributed to depleting the battery life. Breaking up the vertical profile to change the battery did not seem to affect the measurements, which bodes well for applying this method to higher altitude UAV flights. It could still be possible make a slow continuous ascent to 1000 m with a fast descent on one set of batteries, but then the sensor's measurement period and sensitivity to changing environmental conditions should be taken into consideration. A benefit of UAVs in comparison to manned aircraft is that the altitude and air speed can be more carefully controlled, which is preferred for instruments with a lower time resolution and which are sensitive to fluctuations in air speed.

Placement of sensors above or below the body of the UAV and length of inlet (if used) was found to vary between different studies. The most practical way to attach the Partector 2 and MA300 was to the underside of the drone using a ventilated and padded box, which also helped to minimise vibrations to which the instruments can be sensitive to. The top-placement of the OPC-N3 due to its inability to sample from an inlet did not seem to have noticeable consequences on the data, but it may have experienced extra warming from the sun which can be a problem for sensors in that position. Based on prior studies using bigger UAVs (Pikridas et al., 2019; Haugen et al., 2022), the 95 cm inlet used in

this set-up was believed to be sufficient even without more comprehensive testing of the extent of the downwash. This was confirmed by the good agreement between the sensors and reference instruments while hovering at 30 m (Figure 6, Figure 7, and Figure 8).

The set-up of sensors on board the manned aircraft was easier in the sense that payload weight was not so restricted, and less manpower was required as the flights were already being made. This allowed for the use of a dryer and the 11-D which could be connected in line with the Partector 2 and MA300. However, an isokinetic inlet typically used in research aircraft measuring aerosols was not possible in this set-up due to use of instructional planes. It is likely there were particle losses within the wing of the plane as the air flowed into the cabin, but the results of this project suggest that this set-up could be good enough.

Since the sensors were placed on planes used in instructional flights with predefined flight strategies, the altitude variations and air speed were not controlled with the aerosol measurements in mind. This was a compromise made in favour of data collection, but something to consider if this method of 'passive' aerosol sampling were to be used in the future. It would be preferable to measure on planes which reach higher altitudes and cover longer distances, and to avoid those which have very fast ascent and descent or in which the route involves circling into the plane's own exhaust plume. An additional improvement to plane-based measurements would be more accurate recording of the altitude for use in profiling. Planes typically have a barometric altimeter onboard which measures the outside pressure to give an indication of the aircraft's altitude above mean sea level, but since meteorology can also affect the ambient pressure a GPS reading would be more appropriate.

5.5 Vertical profile data in models

Atmospheric and global climate models need measurements for validation and improvement, and can also identify new areas in which observations are lacking. The vertical resolution of Earth System Models in the Coupled Model Intercomparison Project phase 6 (CMIP6) presented in AR6 has generally increased since the previous CMIP5 (Chen et al., 2021). At the same time, the uncertainty in the degree to which aerosol-radiation and aerosol-cloud interactions effect radiative forcing has reduced since the previous report, but still represents the largest source of uncertainty of calculations of contributions to change in global surface temperature (Chen et al., 2021). This highlights the importance of collecting aerosol data in the vertical dimension for improving models, future climate scenarios, and decision-making.

Aerosol vertical profiling campaigns seem to be increasing, but measurements need to

be performed all around the world to encapsulate different regional patterns in global models. For example, Heald et al. (2011) used organic aerosol measurements from 17 aircraft campaigns around the world to evaluate a global model. It was found that the model often underestimated values in simulated vertical profiles, and concluded with a need for more data in several regions. Regionally-specific examples include Cappelletti et al. (2022), which produced a set of homogenised gridded data (vertical profiles of BC and nanoparticle concentration and environmental variables) for use in modelling Arctic pollution. Additionally, vertical profiles over three Italian basin valleys were used to produce a model which could predict particle properties with height and estimate the vertical dimension of the aerosol direct radiative effect, amongst other things (Ferrero et al., 2014). While both of these studies used measurements from tethered-balloons, UAV-based measurement could surely be used in similar ways.

Chapter 6

Conclusions

- The Partector 2, MA300, and OPC-N3 compared well overall against the reference instruments MPSS, AE33, and Fidas 200 in measurements of total number, BC, and PM2.5 concentrations. During three periods of comparison, a significant difference between the mean of the data from the portable sensor and that of the reference instrument was only found in 2 of 8 cases.
- The Partector 2 and MA300 are suited well to use on UAV and aircraft platforms. They can be connected to inlets (also allowing for a dryer to be used), and their air flow is controlled by pumps. The OPC-N3, despite its size and low-cost being attractive for UAV applications, is limited by its fan and susceptibility to RH errors. The 11-D spectrometer worked well on the aircraft, but its higher weight and cost mean it is not a good candidate for UAV measurements.
- The UAV-based vertical profiles within the lowest 120–165 m of the atmosphere showed a well mixed aerosol. The concentration of particle number, BC, and PM2.5 decreased with altitude during aircraft-based measurements, and a notable drop above 1500 m seemed to indicate the plane crossing the PBL.
- The hypothesised difference between vertical aerosol concentrations within and outside of the forest canopy was not observed within this project.

6.1 Outlook

The results of this thesis project affirm the compatibility of several portable aerosol sensors with unmanned and manned aircraft, but also highlight areas for improvement in future vertical profiling studies.

In order to collect data for model evaluation and improvement, repeating the vertical profile measurements throughout more seasons and over a longer time would be required. Measuring a larger sample size in a wider variation of air masses and atmospheric conditions would help improve understanding of the links between vertical concentration gradients and meteorological factors. Once the permit situation allows for high altitude UAV flights, the ability to sample aerosols with high temporal and vertical spatial resolution is expected to be very useful for atmospheric research and modelling. With higher altitude and lengthened drone measurement campaigns, all sensors would benefit from a dryer connected to the sampling inlet. For example, AethLabs's Portable Aerosol Dryer with a weight of 128 g could be an option suitable for UAV applications. Additionally,

much more flexibility for obtaining measurements would be gained if researchers underwent training to pilot the UAV independently.

The access to routine manned flights represents a great opportunity for more aerosol measurements at altitude in the future. Duplicate sets of sensors installed on more plane would take even better advantage of these flights. The set-up would additionally be improved with an isokinetic inlet and a more direct sampling of outside air than through the wing, plus a GPS altimeter and ambient sensors for temperature, pressure, and RH. This project suggested vertical profile measurements are best focused on flights reaching high altitudes with longer and continuous ascent and descent. However, having a more permanent implementation of sensors on one or more planes could produce large datasets with minimal man-power. Streamlining the post-processing of aerosol measurements and flight details, for example with machine learning algorithms, would greatly assist in the usability of the data.

Bibliography

Aitken, J. (1890). On the Number of Dust Particles in the Atmosphere of certain Places in Great Britain and on the Continent, with Remarks on the Relation between the Amount of Dust and Meteorological Phenomena. *Proceedings of the Royal Society of Edinburgh*, 17.

Allen, S., D. Allen, F. Baladima, V. Phoenix, J. Thomas, G. Le Roux, and J. Sonke (Dec. 2021). Evidence of free tropospheric and long-range transport of microplastic at Pic du Midi Observatory. *Nature Communications*, 12. DOI: 10.1038/s41467-021-27454-7.

Alvarado, M., L. Gonzalez, P. Erskine, D. Cliff, and D. Heuff (Mar. 2017). A Methodology to Monitor Airborne PM 10 Dust Particles Using a Small Unmanned Aerial Vehicle. *Sensors*, 17. DOI: 10.3390/s17020343.

Bezantakos, S., M. Costi, K. Barmpounis, P. Antoniou, C. Keleshis, J. Sciare, and G. Biskos (2020). Qualification of the Alphasense optical particle counter for inline air quality monitoring. *Aerosol Science and Technology*, 55. DOI: 10.1080/02786826.2020.1864276.

Bezantakos, S., F. Schmidt-Ott, and G. Biskos (2018). Performance evaluation of the cost-effective and lightweight Alphasense optical particle counter for use onboard unmanned aerial vehicles. *Aerosol Science and Technology*, 52: 385–392. DOI: 10.1080/02786826.2017.1412394.

Boucher, O. (2015). *Atmospheric Aerosols*. Paris, France: Springer. ISBN: 978-94-017-9648-4. DOI: 10.1007/978-94-017-9649-1.

Brus, D., J. Gustafsson, V. Vakkari, O. Kemppinen, G. de Boer, and A. Hirsikko (2021). Measurement report: Properties of aerosol and gases in the vertical profile during the LAPSE-RATE campaign. *Atmospheric Chemistry and Physics*, 21: 517–533. DOI: 10.5194/acp-21-517-2021.

Cappelletti, D., C. Petroselli, D. Mateos, M. Herreras, L. Ferrero, N. Losi, A. Gregorič, C. Frangipani, et al. (2022). Vertical profiles of black carbon and nanoparticles pollutants measured by a tethered balloon in Longyearbyen (Svalbard islands). *Atmospheric Environment*, 290. DOI: 10.1016/j.atmosenv.2022.119373.

Chen, D., M. Rojas, B. H. Samset, K. Cobb, A. Diongue Niang, P. Edwards, S. Emori, S. H. Faria, et al. (2021). "Framing, Context, and Methods". In: *Climate Change 2021: The Physical Science Basis. Contribution of Working Group I to the Sixth Assessment Report of the Intergovernmental Panel on Climate Change*. Ed. by V. Masson-Delmotte, P. Zhai, A. Pirani, S. L. Connors, C. Péan, S. Berger, N. Caud, Y. Chen, et al. Cambridge, United Kingdom and New York, NY, USA: Cambridge University Press. Chap. 1.

Chilinski, M. T., K. M. Markowicz, and J. Markowicz (2016). Observation of vertical variability of black carbon concentration in lower troposphere on campaigns in Poland. *Atmospheric Environment*, 137: 155–170. DOI: 10.1016/j.atmosenv.2016.04.020.

Chiliński, M., K. Markowicz, and M. Kubicki (Sept. 2018). UAS as a Support for Atmospheric Aerosols Research: Case Study. *Pure and Applied Geophysics*, 175. DOI: 10.1007/s00024-018-1767-3.

Corrigan, C. E., G. C. Roberts, M. V. Ramana, D. Kim, and V. Ramanathan (2008). Capturing vertical profiles of aerosols and black carbon over the Indian Ocean using autonomous unmanned aerial vehicles. *Atmospheric Chemistry and Physics*, 8: 737–747. DOI: 10.5194/acp-8-737-2008.

Drinovec, L., G. Močnik, P. Zotter, A. S. H. Prévôt, C. Ruckstuhl, E. Coz, M. Rupakheti, J. Sciare, et al. (2015). The "dual-spot" Aethalometer: an improved measurement of aerosol

black carbon with real-time loading compensation. *Atmospheric Measurement Techniques*, 8: 1965–1979. DOI: 10.5194/amt-8-1965-2015.

Fan, J., Y. Wang, D. Rosenfeld, and X. Liu (2016). Review of Aerosol-Cloud Interactions: Mechanisms, Significance, and Challenges. *Journal of the Atmospheric Sciences*, 73: 4211–4252. DOI: https://doi.org/10.1175/JAS-D-16-0037.1.

Ferrero, L., M. Castelli, B. S. Ferrini, M. Moscatelli, M. G. Perrone, G. Sangiorgi, L. D'Angelo, G. Rovelli, et al. (2014). Impact of black carbon aerosol over Italian basin valleys: high-resolution measurements along vertical profiles, radiative forcing and heating rate. *Atmospheric Chemistry and Physics*, 14: 9641–9664. DOI: 10.5194/acp-14-9641-2014.

Fierz, M., D. Meier, P. Steigmeier, and H. Burtscher (2014). Aerosol Measurement by Induced Currents. *Aerosol Science and Technology*, 48: 350–357. DOI: 10.1080/02786826.2013.875981.

Hansen, A., H. Rosen, and T. Novakov (1984). The aethalometer — An instrument for the real-time measurement of optical absorption by aerosol particles. *Science of The Total Environment*, 36: 191–196. DOI: 10.1016/0048-9697(84)90265-1.

Haugen, M. J., S. Gkantonas, I. El Helou, R. Pathania, E. Mastorakos, and A. M. Boies (2022). Measurements and modelling of the three-dimensional near-field dispersion of particulate matter emitted from passenger ships in a port environment. *Atmospheric Environment*, 290. DOI: 10.1016/j.atmosenv.2022.119384.

Heald, C. L., H. Coe, J. L. Jimenez, R. J. Weber, R. Bahreini, A. M. Middlebrook, L. M. Russell, M. Jolleys, et al. (2011). Exploring the vertical profile of atmospheric organic aerosol: comparing 17 aircraft field campaigns with a global model. *Atmospheric Chemistry and Physics*, 11: 12673–12696. DOI: 10.5194/acp-11-12673-2011.

Hedworth, H. A., T. Sayahi, K. E. Kelly, and T. Saad (2021). The effectiveness of drones in measuring particulate matter. *Journal of Aerosol Science*, 152. DOI: 10.1016/j.jaerosci.2020.105702.

Hinds, W. C. (1982). *Aerosol Technology*. United States of America: John Wiley & Sons, Inc.

IPCC (2013). *Climate Change 2013 The Physical Science Basis*. Intergovernmental Panel on Climate Change. ISBN: 978-92-9169-138-8.

Järvi, L., M. Kurppa, H. Kuuluvainen, T. Rönkkö, S. Karttunen, A. Balling, H. Timonen, J. V. Niemi, et al. (2023). Determinants of spatial variability of air pollutant concentrations in a street canyon network measured using a mobile laboratory and a drone. *Science of The Total Environment*, 856. DOI: 10.1016/j.scitotenv.2022.158974.

Kipling, Z., P. Stier, C. E. Johnson, G. W. Mann, N. Bellouin, S. E. Bauer, T. Bergman, M. Chin, et al. (2016). What controls the vertical distribution of aerosol? Relationships between process sensitivity in HadGEM3–UKCA and inter-model variation from AeroCom Phase II. *Atmospheric Chemistry and Physics*, 16: 2221–2241. DOI: 10.5194/acp-16-2221-2016.

Kuuluvainen, H., M. Poikkimäki, A. Järvinen, J. Kuula, M. Irjala, M. Dal Maso, J. Keskinen, H. Timonen, et al. (2018). Vertical profiles of lung deposited surface area concentration of particulate matter measured with a drone in a street canyon. *Environmental Pollution*, 241: 96–105. DOI: 10.1016/j.envpol.2018.04.100.

Kwak, K., S. Lee, A. Kim, K. Park, S. Lee, B. Han, J. Lee, and Y. Park (2020). Daytime Evolution of Lower Atmospheric Boundary Layer Structure: Comparative Observations between a 307-m Meteorological Tower and a Rotary-Wing UAV. *Atmosphere*, 11.

Li, X., D. Wang, Q. Lu, Z. Peng, and Z. Wang (2018). Investigating vertical distribution patterns of lower tropospheric PM2.5 using unmanned aerial vehicle measurements. *Atmospheric Environment*, 173: 62–71. DOI: 10.1016/j.atmosenv.2017.11.009.

Li, Z., J. Guo, A. Ding, H. Liao, J. Liu, Y. Sun, T. Wang, H. Xue, et al. (2017). Aerosol and boundary-layer interactions and impact on air quality. *National Science Review*, 4: 810–833. DOI: 10.1093/nsr/nwx117.

Liu, B., C. Wu, N. Ma, Q. Chen, Y. Li, J. Ye, S. T. Martin, and Y. J. Li (2020). Vertical profiling of fine particulate matter and black carbon by using unmanned aerial vehicle in Macau, China. *Science of the Total Environment*, 709. DOI: 10.1016/j.scitotenv.2019.136109.

Liu, X., H. Hadiatullah, X. Zhang, L. D. Hill, A. H. A. White, J. Schnelle-Kreis, J. Bendl, G. Jakobi, et al. (2021). Analysis of mobile monitoring data from the microAeth® MA200 for measuring changes in black carbon on the roadside in Augsburg. *Atmospheric Measurement Techniques*, 14: 5139–5151. DOI: 10.5194/amt-14-5139-2021.

Liu, Z., M. Osborne, K. Anderson, J. D. Shutler, A. Wilson, J. Langridge, S. H. L. Yim, H. Coe, et al. (2021). Characterizing the performance of a POPS miniaturized optical particle counter when operated on a quadcopter drone. *Atmospheric Measurement Techniques*, 14: 6101–6118. DOI: 10.5194/amt-14-6101-2021.

Mahilang, M., M. K. Deb, and S. Pervez (2021). Biogenic secondary organic aerosols: A review on formation mechanism, analytical challenges and environmental impacts. *Chemosphere*, 262: 127771. DOI: 10.1016/j.chemosphere.2020.127771.

Mamali, D., E. Marinou, J. Sciare, M. Pikridas, P. Kokkalis, M. Kottas, I. Binietoglou, A. Tsekeri, et al. (2018). Vertical profiles of aerosol mass concentration derived by unmanned airborne in situ and remote sensing instruments during dust events. *Atmospheric Measurement Techniques*, 11 (5): 2897–2910. DOI: 10.5194/amt-11-2897-2018.

Mishra, A. K., I. Koren, and Y. Rudich (2015). Effect of aerosol vertical distribution on aerosol-radiation interaction: A theoretical prospect. *Heliyon*, 1. DOI: 10.1016/j.heliyon.2015.e00036.

Molero, F., A. J. Fernández, M. A. Revuelta, I. Martínez-Marco, M. Pujadas, and B. Artíñano (2021). Effect of Vertical Profile of Aerosols on the Local Shortwave Radiative Forcing Estimation. *Atmosphere*, 12. DOI: 10.3390/atmos12020187.

Nurowska, K., M. Mohammadi, S. Malinowski, and K. Markowicz (2022). Applicability of the low-cost optical particle counter OPC-N3 for microphysical measurements of fog. *Atmospheric Measurement Techniques Discussions*, 2022: 1–25. DOI: 10.5194/amt-2022-269.

Penner, J., M. Andreae, H. Annegarn, L. Barrie, J. Feichter, D. Hegg, A. Jayaraman, R. Leaitch, et al. (2021). "Aerosols, their Direct and Indirect Effects". In: *Climate Change 2001: The Scientific Basis. Contribution of Working Group I to the Third Assessment Report of the Intergovernmental Panel on Climate Change*. Cambridge, United Kingdom and New York, NY, USA: Cambridge University Press. Chap. 5.

Petzold, A., V. Thouret, C. Gerbig, A. Zahn, C. A. M. Brenninkmeijer, M. Gallagher, M. Hermann, M. Pontaud, et al. (2015). Global-scale atmosphere monitoring by in-service aircraft – current achievements and future prospects of the European Research Infrastructure IAGOS. *Tellus B: Chemical and Physical Meteorology*, 67 (1).

Pikridas, M., S. Bezantakos, G. Močnik, C. Keleshis, F. Brechtel, I. Stavroulas, G. Demetriades, P. Antoniou, et al. (2019). On-flight intercomparison of three miniature aerosol absorption

sensors using unmanned aerial systems (UASs). *Atmospheric Measurement Techniques*, 12: 6425–6447. DOI: 10.5194/amt-12-6425-2019.

Quan, J., Y. Gao, Z. Qiang, X. Tie, J. Cao, S. Han, J. Meng, P. Chen, et al. (Jan. 2012). Evolution of Planetary Boundary Layer under different weather conditions, and its impact on aerosol concentrations. *Particuology*, 11. DOI: 10.1016/j.partic.2012.04.005.

Ran, L., Z. Deng, X. Xu, P. Yan, W. Lin, Y. Wang, P. Tian, P. Wang, et al. (2016). Vertical profiles of black carbon measured by a micro-aethalometer in summer in the North China Plain. *Atmospheric Chemistry and Physics*, 16: 10441–10454. DOI: 10.5194/acp-16-10441-2016.

Reddy, K., D. Phanikumar, Y. Ahammed, and M. Naja (Oct. 2013). Aerosol vertical profiles strongly affect their radiative forcing uncertainties: Study by using ground based lidar and other measurements. *Remote Sensing Letters*, 4. DOI: 10.1080/2150704X.2013.828182.

Rolph, G., A. Stein, and B. Stunder (2017). Real-time Environmental Applications and Display sYstem: READY. *Environmental Modelling & Software*, 95: 210–228. DOI: 10.1016/j.envsoft.2017.06.025.

Shao, J., F. Yi, and Z. Yin (2020). Aerosol layers in the free troposphere and their seasonal variations as observed in Wuhan, China. *Atmospheric Environment*, 224: 117323. DOI: https://doi.org/10.1016/j.atmosenv.2020.117323.

Shi, Y., F. Hu, Z. Xiao, G. Fan, and Z. Zhang (2020). Comparison of four different types of planetary boundary layer heights during a haze episode in Beijing. *Science of The Total Environment*, 711. DOI: 10.1016/j.scitotenv.2019.134928.

Soroka, E. (2020). *Indoor and Outdoor Measurements of Particulate Matter with the Low-Cost Optical Sensor OPC-N3*. Bachelor Thesis. Lund, Sweden: Lund University. URL: http://lup.lub.lu.se/student-papers/record/9017097.

Stein, A. F., R. R. Draxler, G. D. Rolph, B. J. B. Stunder, M. D. Cohen, and F. Ngan (2015). NOAA's HYSPLIT Atmospheric Transport and Dispersion Modeling System. *Bulletin of the American Meteorological Society*, 96: 2059–2077. DOI: 10.1175/BAMS-D-14-00110.1.

Su, T., Z. Li, C. Li, J. Li, W. Han, C. Shen, W. Tan, J. Wei, et al. (2020). The significant impact of aerosol vertical structure on lower atmosphere stability and its critical role in aerosol–planetary boundary layer (PBL) interactions. *Atmospheric Chemistry and Physics*, 20 (6): 3713–3724. DOI: 10.5194/acp-20-3713-2020.

Uno, I., K. Eguchi, K. Yumimoto, T. Takemura, A. Shimizu, M. Uematsu, Z. Liu, Z. Wang, et al. (July 2009). Asian dust transported one full circuit around the globe. *Nature Geoscience*, 2. DOI: 10.1038/NGEO583.

Villa, T. F., F. Gonzalez, B. Miljievic, Z. D. Ristovski, and L. Morawska (2016). An Overview of Small Unmanned Aerial Vehicles for Air Quality Measurements: Present Applications and Future Prospectives. *Sensors*, 16. DOI: 10.3390/s16071072.

Wu, C., B. Liu, D. Wu, H. Yang, X. Mao, J. Tan, Y. Liang, J. Y. Sun, et al. (2021). Vertical profiling of black carbon and ozone using a multicopter unmanned aerial vehicle (UAV) in urban Shenzhen of South China. *Science of the Total Environment*, 801. DOI: 10.1016/j.scitotenv.2021.149689.

Appendices

A Pictures of set-up

(a) Front (b) Back (c) Partector 2 and MA300 inside the padded box.

Figure A.1: Closer look at the drone and sensor set up.

Figure A.2: Cirrus SR-20 aircraft.

Figure A.3: Sensor set up on the back seat of the aircraft, with the common inlet to the sensors fed into the air outlet.

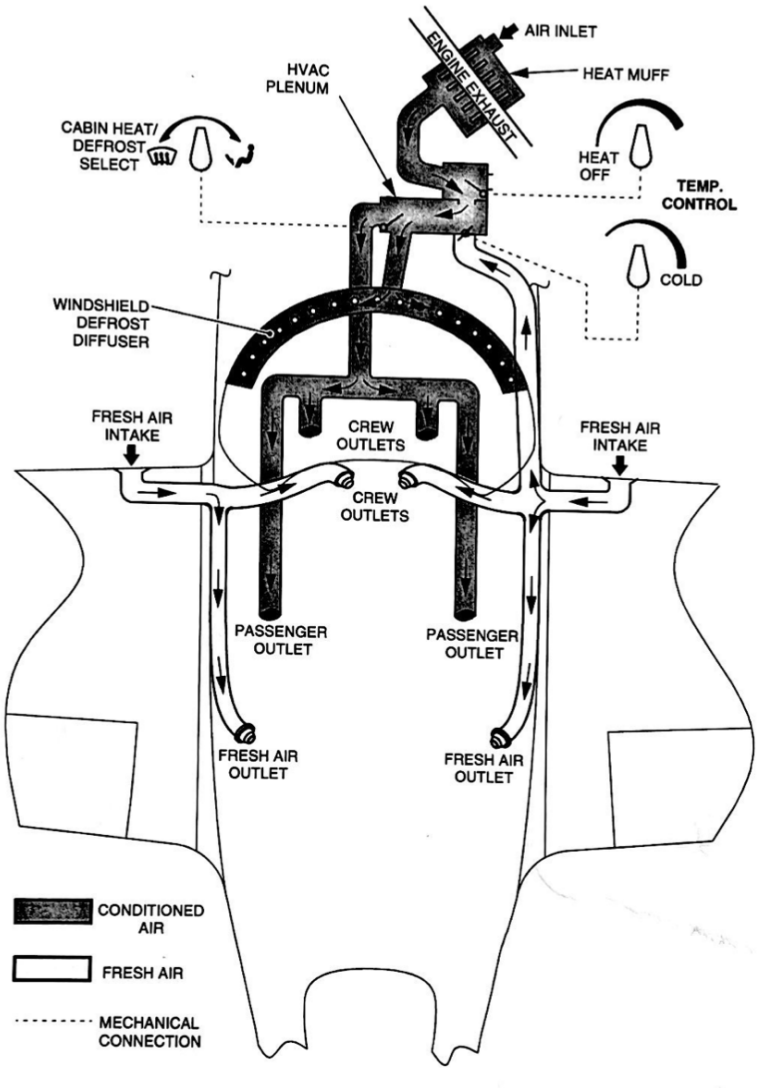

Figure A.4: Cirrus SR-20 heating and ventilation. Figure taken from the Cirrus Design SR20 Handbook with permission.

B Supplementary figures

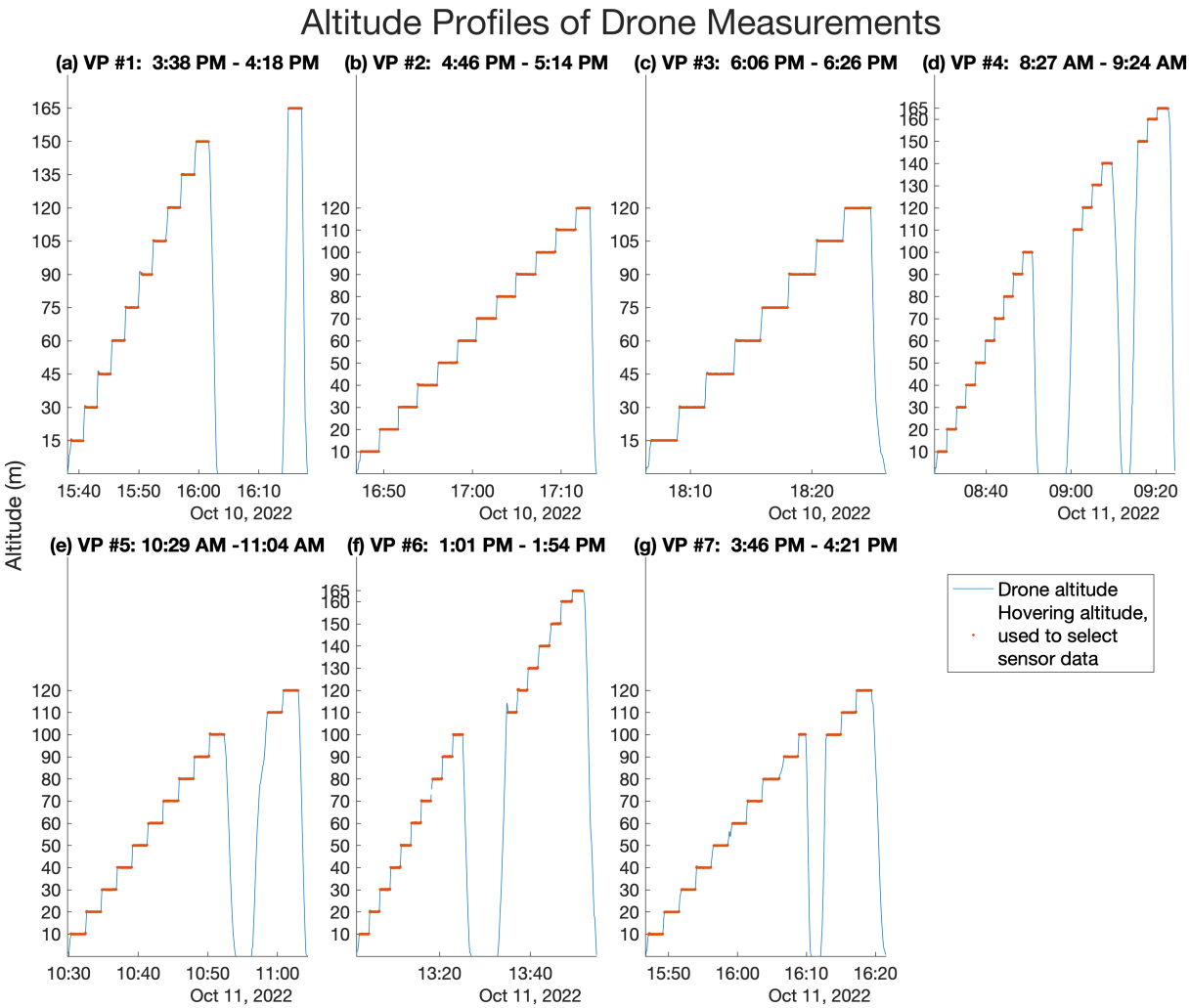

Figure B.1: Time series of the drone altitude during each of the seven vertical profiles, showing the hovering sections used to select the data from the sensors and the breaks when battery change was required.

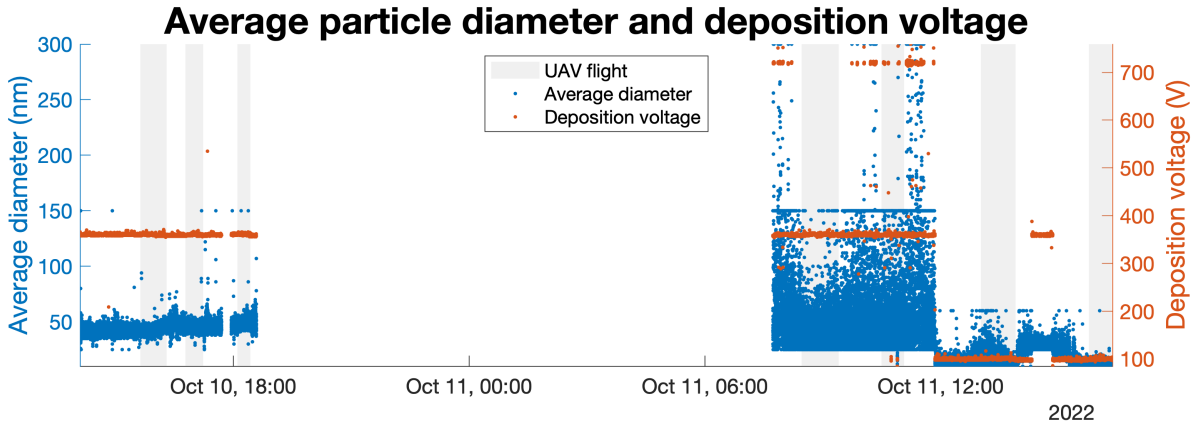

Figure B.2: Average particle diameter and deposition voltage measurements for the entire set of Partector 2 data. Periods of UAV flights are shaded.

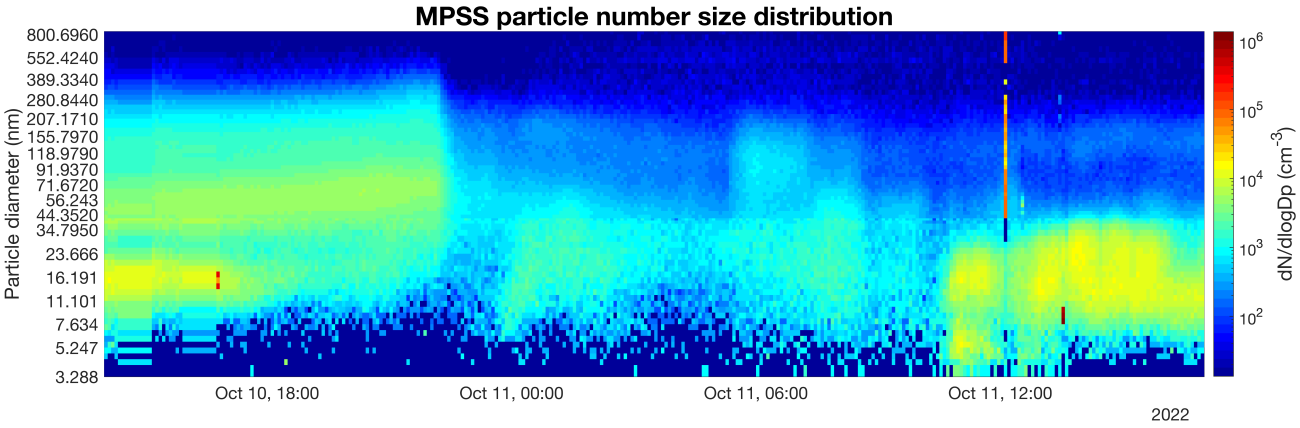

Figure B.3: Particle number size distribution measured by the MPSS during 10–11th October

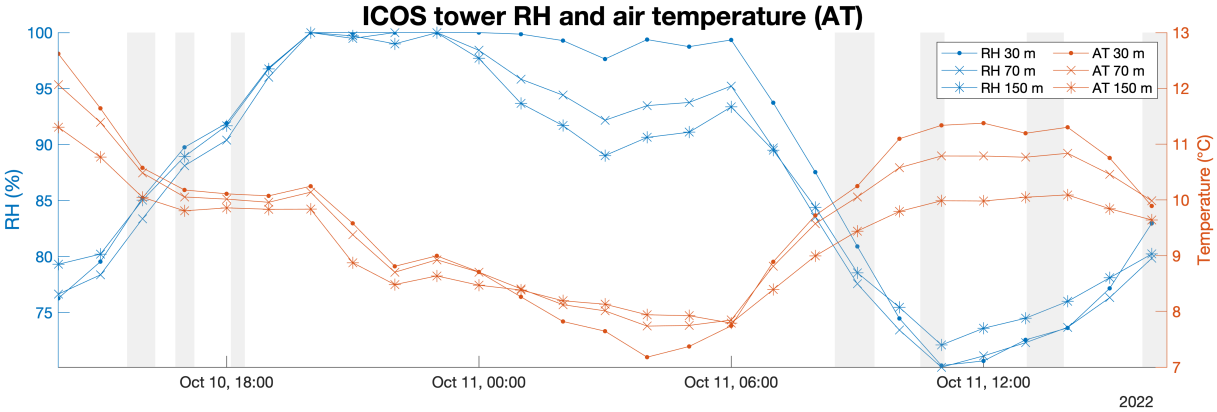

Figure B.4: RH and temperature recorded on the ICOS tower at 30, 70 and 150 m.

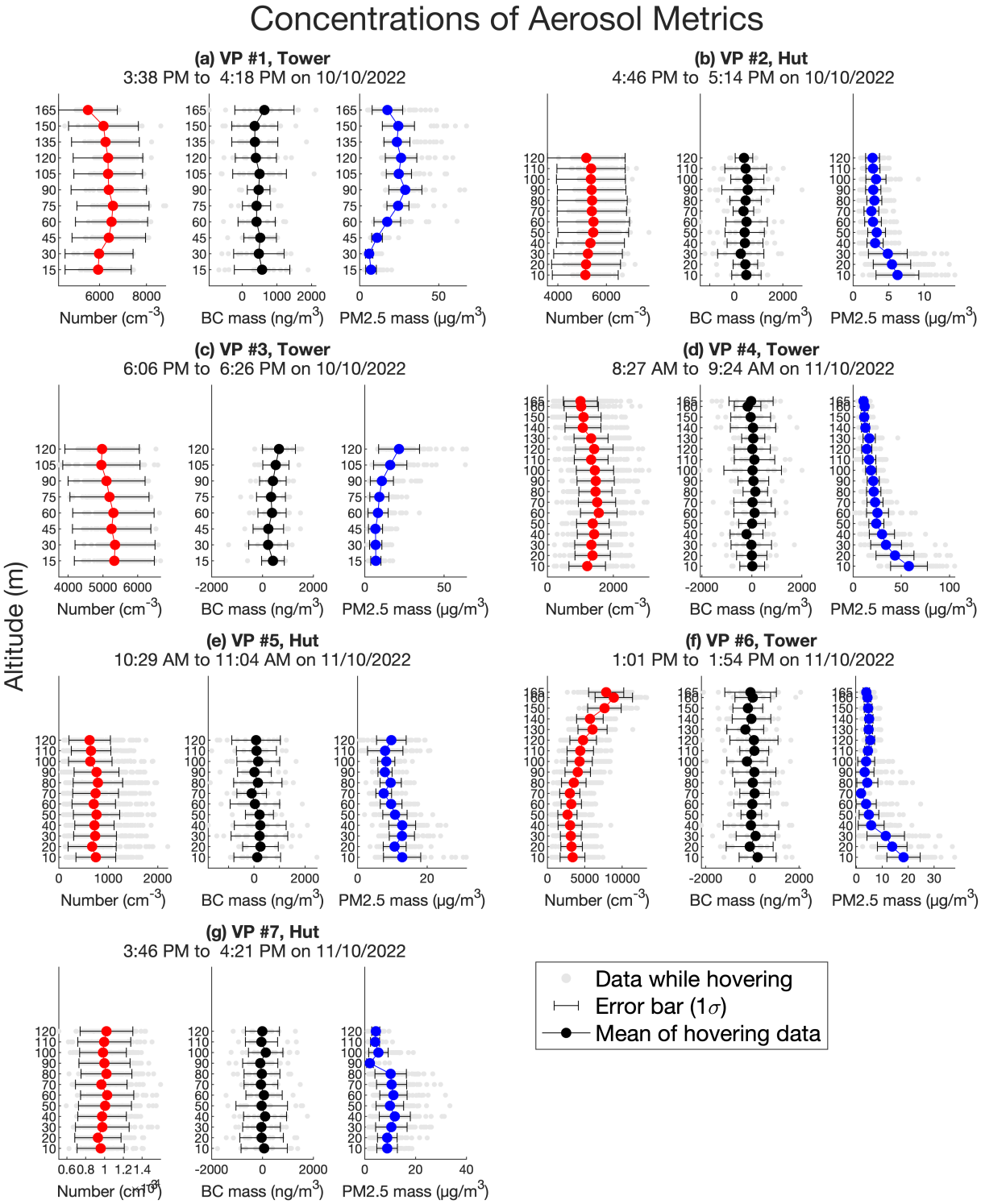

Figure B.5: Vertical profiles of the mean total number, BC mass, and PM2.5 mass concentration during each hovering altitude, in chronological order of UAV flights. Error bars of one standard deviation and the total spread of data points while hovering are included.

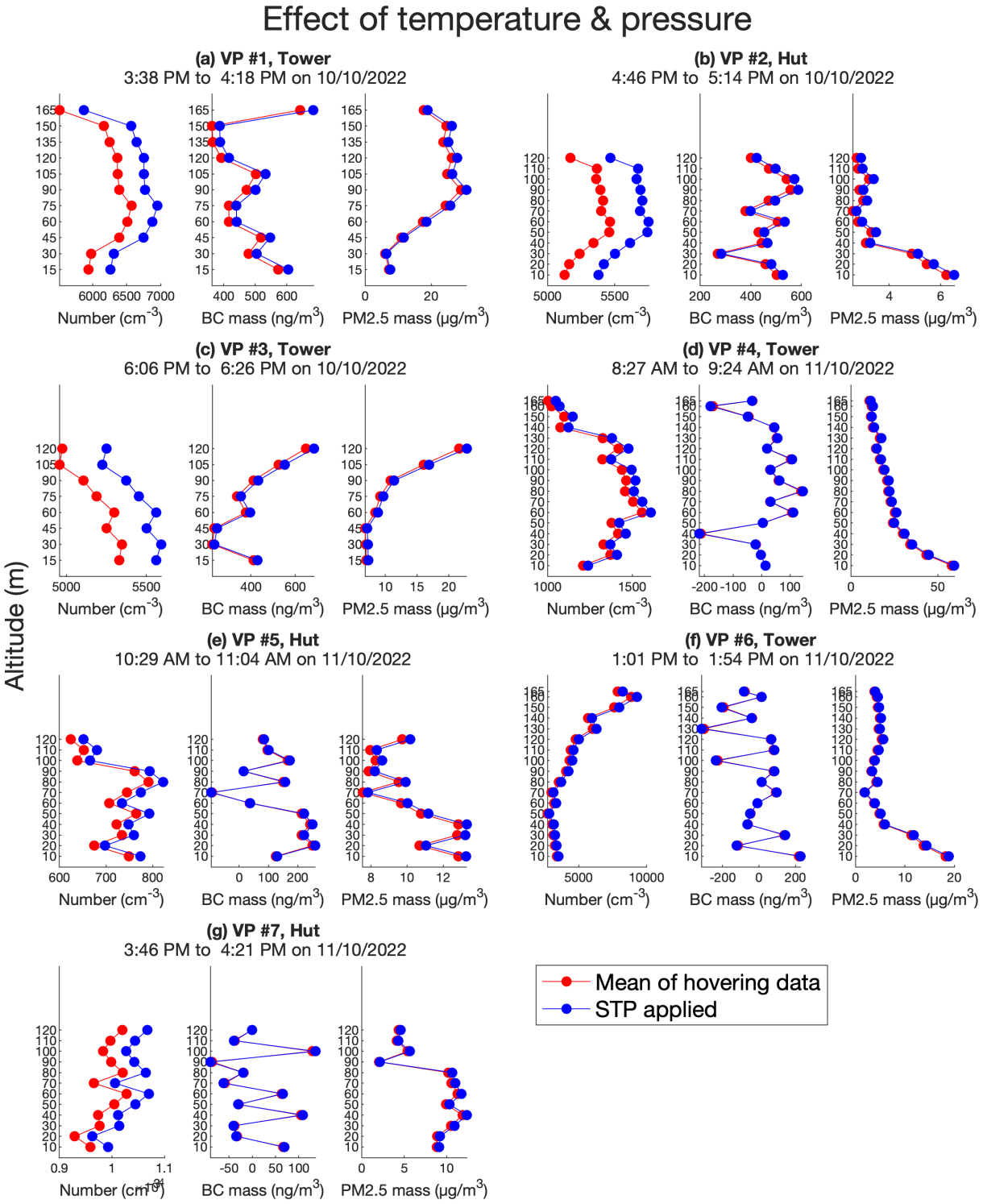

Figure B.6: Vertical profiles with and without STP conversion using temperature and pressure from the Sparvio sensors.

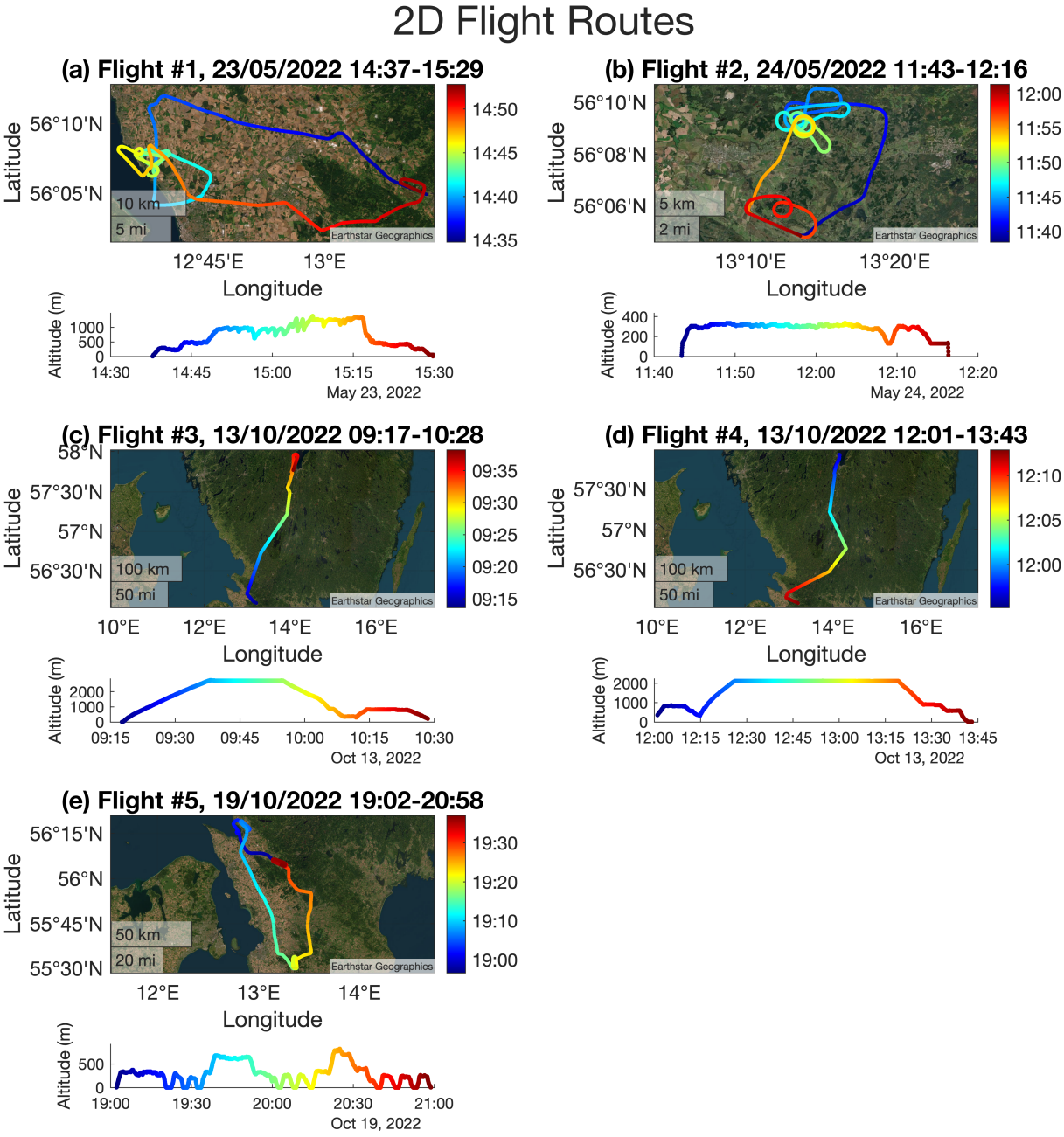

Figure B.7: 2D routes of the five flights carrying aerosol sensors, with the corresponding time and altitude timeseries.

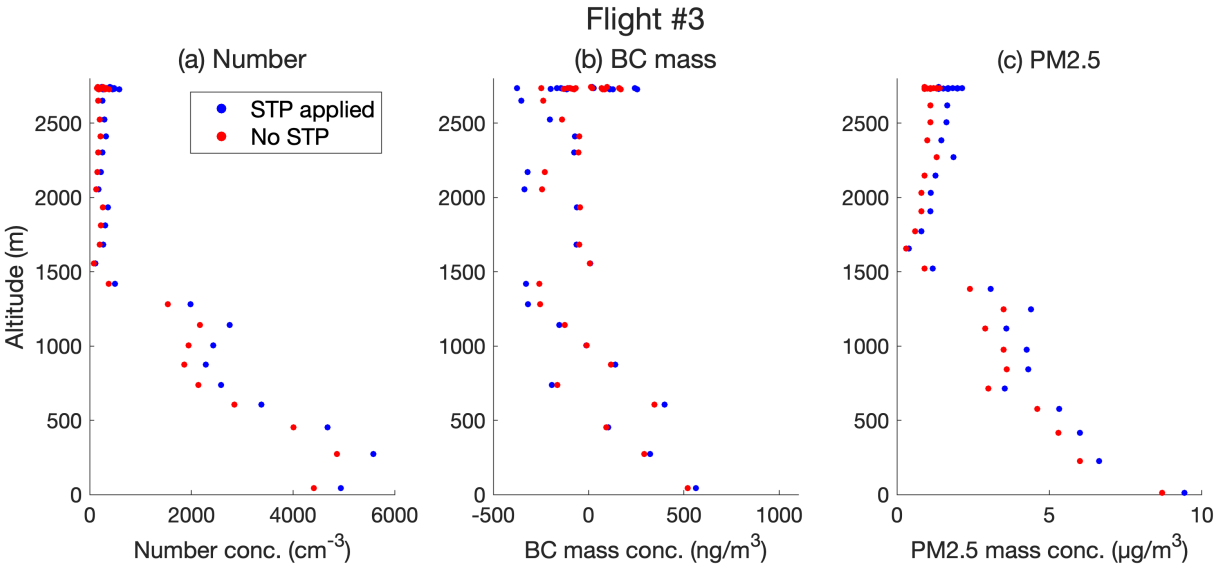

Figure B.8: Example from flight #3 showing vertical profiles of (a) total particle number, (b) BC mass, and (c) PM2.5 mass concentrations with and without STP conversion. The temperature and pressure measured internally by each respective sensor was used for conversion.